COMPUTATIONAL MODEL TO DETERMINE TIBIOFEMORAL FORCES AND MOMENTS DURING KNEELING

by

Jonisha P. Pollard

B.S., University of Pittsburgh, 2005

Submitted to the Graduate Faculty of

the Swanson School of Engineering in partial fulfillment

of the requirements for the degree of

Master of Science

University of Pittsburgh

2008

UNIVERSITY OF PITTSBURGH

SWANSON SCHOOL OF ENGINEERING

This thesis was presented

by

Jonisha P. Pollard

It was defended on

November 11, 2008

and approved by

Jean L. McCrory, PhD, Research Assistant Professor, Health and Physical Activity

Richard E. Debski, PhD, Associate Professor, Department of Bioengineering

Rakié Cham, PhD, Associate Professor, Department of Bioengineering

Thesis Advisor: Mark S. Redfern, PhD, Professor, Department of Bioengineering, Associate Dean for Research

COMPUTATIONAL MODEL TO DETERMINE TIBIOFEMORAL FORCES AND MOMENTS DURING KNEELING

Jonisha P. Pollard, M.S.

University of Pittsburgh, 2008

Osteoarthritis affects more than 27 million Americans and cost nearly $5700 per person annually. [1, 2] It commonly affects the knee joint and has been linked to work involving prolonged knee bending. [3, 4] In restricted vertical working heights such as low-seam coal mines and aircraft baggage compartments, workers are forced to assume stooped, kneeling, or squatting postures to perform work. In order to protect the knees in these postures, we must have an understanding of what the internal knee structures experience under these conditions. A finite element model is being developed to quantify the stresses and strains in the tissues in static kneeling postures. The accuracy of any finite element model is heavily dependent on the input parameters (i.e. forces and moments). Therefore, the objective of this work was to develop a 3-D computational model which may be used to determine the net forces and moments applied to the knee joint during static kneeling. The developed model uses inverse dynamics to determine the net forces, net moments, and joint angles for subjects while kneeling near full flexion, kneeling on one knee, kneeling near 90° flexion, and squatting. Motion data, ground reaction forces, and pressures between the thigh and calf and heel and gluteal muscles were inputs into this model. Additionally the thigh-calf contact force, which was shown to be significant [5], and the heel-gluteus contact force, which had not been previously investigated, were inputs in this model. Data from two subjects were analyzed with and without the subject wearing kneepads. Kneeling near full flexion and squatting created sagittal joint moments 3 to 5 times larger than standing in

one subject. Moments of this magnitude may be significant to cause cartilage damage. It was also found that the moments caused by the thigh-calf and heel-gluteus contacts act to extend the knee, thereby reducing knee moments in fully flexed postures.

TABLE OF CONTENTS

LIST OF TABLES

LIST OF FIGURES

NOMENCLATURE

COM – Center of mass

COP – Center of pressure

KJC – Knee joint center

AJC – Ankle joint center

HJC – Hip joint center

ATCS – Anatomical thigh coordinate system

ASCS – Anatomical shank coordinate system

GCS – Global coordinate system

MCS – Measured coordinate system

MSCS – Measured shank coordinate system

MTCS – Measured thigh coordinate system

$F_{t/c}$ – Thigh-calf contact force

$F_{h/g}$ – Heel-gluteus contact force

T_{TGA} – Transformation matrix from ATCS to GCS

T_{SGA} – Transformation matrix from ASCS to GCS

T_{TMA} – Transformation matrix from ATCS to MTCS

T_{SMA} – Transformation matrix from ASCS to MSCS

T_{ST} – Transformation matrix from ATCS to ASCS

F_{knee} – Net external force applied to the knee

M_{knee} – Net external moment applied to the knee

1.0 INTRODUCTION

Osteoarthritis affects more than 27 million Americans and cost nearly $5700 per person annually. [1, 2] Certain occupational activities as well as heredity, age, trauma, or repetitive stress have been associated with osteoarthritis in the knee. Studies have suggested that the risk of developing knee osteoarthritis is increased by work involving prolonged knee bending. [3, 4]

A large project is underway at the NIOSH Pittsburgh Research Laboratory to gain a better understanding of the biomechanics of the knee joint while kneeling, squatting, and crawling in order to develop guidelines for the manufacture of kneepads, which may be used to alleviate stress while kneeling. Subjects will assume kneeling postures typically seen in the mining industry. Kinematics and kinetics data (motion capture, force plate, electromyography, and pressure sensor) will be collected. The ultimate goal of the project is to develop a finite element model of the knee in kneeling postures, which will provide a further understanding of the biomechanics of knee structures while kneeling and crawling.

The goal of this Master's thesis project was to develop a computational model which will be used to determine the dynamic net forces and moments imposed on the knee joint during static kneeling postures with and without knee pads. Motion data, force plate data, and pressure sensor data were inputs into this model. The results of this thesis work will be incorporated in the finite element model.

1.1 BACKGROUND

Musculoskeletal disorders vary by occupation. Different jobs expose workers to differing ergonomic risk factors. People who work in restricted spaces, such as underground coal mines or aircraft baggage compartments, are forced to assume awkward postures (such as kneeling, stooping, and crawling) due to the restricted vertical height of their working environment. Other occupations such as plumbers, carpet layers, roofers, housemaids, and agricultural workers may not have this restriction in vertical height, but may also assume awkward postures to perform work. This background section focuses on musculoskeletal injuries due to the awkward postures of kneeling and squatting. First, the musculoskeletal structures that are affected by kneeling and squatting are discussed, after which a review of occupational factors related to knee injuries is presented.

1.2 KNEE STRUCTURES AND INJURIES

The knee is a complex weight bearing joint that connects the femur, patella, and tibia forming the patellofemoral and tibiofemoral joints. It is also comprised of various ligaments, tendons, and cartilage that function to add stability, motion, and weight bearing (Figure 1). (For more information on the knee structures and their function see [6]) Any structure of the knee is susceptible to injury; however, many occupational related disorders affect the bursae, meniscus, and cartilage. This is particularly true for knee-straining postures such as kneeling and squatting. [7 - 10]

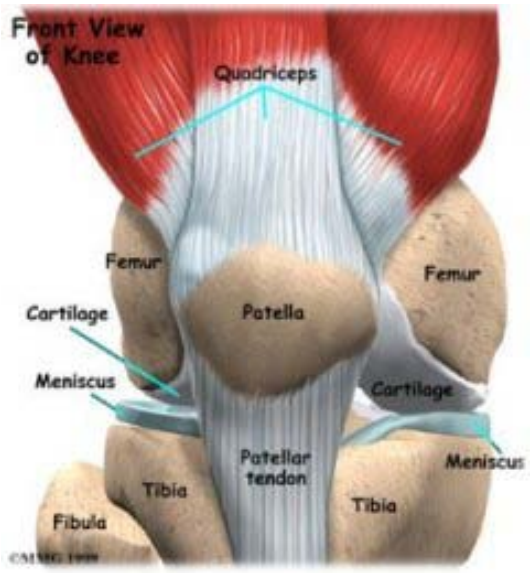

Figure 1: Front view of knee anatomy [11]

The bursa is a fluid filled sac that acts as a cushion between a tendon and a bone or a tendon and a muscle. Within the knee there are numerous bursae, both deep and subcutaneous. There are three large subcutaneous bursae that may become injured from repetitive motions or trauma. The suprapatellar bursa is between the femur and the tendon of the quadriceps femoris muscle. This bursa facilitates full flexion and extension of the knee and may become injured during acute trauma. The prepatellar bursa is between the patellar tendon and the skin. It acts as a cushion, reducing the friction between the patella and the skin while kneeling. The subcutaneous infrapatellar bursa is located between the skin and the tibial tuberosity. It allows the skin to move easily over the tibial tuberosity and withstands pressure when kneeling with the trunk upright. Any of these bursae may become irritated and inflamed, resulting in bursitis. Bursitis generally results in a swollen bursa and restricted joint motion. In some cases the bursa may become infected, resulting in a serious condition, septic bursitis.

The meniscus is a cartilaginous structure that provides a number of basic functions: load bearing, stability, lubrication, and shock absorption. The meniscus transmits between 50-70 %

of the compressive loads in the knee. [12] During the stance phase of gait the mean contact stress on the meniscus is 20 klbs per cm^2. [13] The meniscus provides stability by interacting with the Anterior Cruciate Ligament (ACL), assisting with rotational stability. The meniscus also prevents friction between the femur and tibia and allows diffusion of joint fluid into the articular cartilage. The meniscus increases the load carrying area of the joint by 200 %, thereby lowering the stress applied to the articular cartilage and acting as a shock absorber. [12]

The meniscus can be damaged by both traumatic and degenerative mechanisms. The most common mechanism of traumatic meniscal tear occurs predominantly in athletes when a twisting moment is applied to the weight bearing knee in a semi-flexed position. This form of meniscal tear is commonly concurrent with an ACL injury. [14] Meniscus tears without ACL injury are commonly the result of degeneration of the meniscus. [15]

The articular cartilage is another structure that is commonly injured. Osteoarthritis is a chronic condition characterized by the breakdown of the joint's articular cartilage. This breakdown in cartilage affects the lubrication process within the knee, and results in direct contact between the bones causing stiffness, pain, and loss of motion. It also reduces the shock absorbing capacity of the knee, leading to microfractures of the subchondral bone. [16] Osteoarthritis is the most common joint disorder associated with major disability, affecting more than 27 million Americans. [1, 17, 18] The risk of developing this disease increases with age and it is estimated that by 2030, 20% of Americans (about 72 million people), will be at a high risk for this disease. [18]

1.3 OCCUPATIONAL KNEE INJURIES

Working in certain awkward postures has been to shown to affect musculoskeletal disorders of the lower extremities. [19] Of all lower extremity injuries, knee injuries most commonly result from worker position or motion. [20] Kneeling and crawling can cause knee injuries ranging from minor skin irritations to bursitis or a torn meniscus. [21]

1.3.1 Bursitis

Frequent kneeling produces large stresses on the patella which may thicken the walls of the bursa. [9] This thickening can lead to irritation and inflammation. Prepatellar bursitis is the most common form of bursitis and known as “housemaid’s knee” or “miner’s knee”. While this form of bursitis does not typically lead to other knee injuries, it does account for days lost from work and may lead to infection if left untreated. Bursitis usually does not lead to other knee problems when properly treated.

1.3.2 Meniscal Injuries

Frequent kneeling also has been linked to an increased laxity in the ACL and development of meniscal injuries. Sharrard and Liddell (1962) investigated hospital records of 957 meniscectomies, performed between January 1958 and June 1960, from five hospitals in one of the largest British coalfields. After reviewing records for men between 15 and 64, the authors determined that miners are more likely than others to suffer cartilage damage of any type. Upon interviewing 200 of the men, the authors determined that cartilage tears were more common in

miners who knelt, but the tears normally occurred when walking. To gain a better understanding of why the tears occurred in non-kneeling posture, the authors examined 80 patients with meniscal damage. From these examinations, they determined that ACL laxity resulted from kneeling at work. The authors proposed that this laxity decreases the stability of the knee in non-restricted postures such as standing and walking, leading to meniscal tears.

Along with kneeling, aging plays a role in the development of meniscal injuries. [22], [23] Drosos and Pozo (2004) conducted a study on 392 patients between the ages of 18 and 60 with meniscal injuries from the general population. 32.4% of patients had sports-related meniscal injuries, 38.8% had non-sports-related injuries and 28.8% had no identifiable injury or no identifiable cause of injury. The most frequently reported mechanism of injury for the non-sporting group was rising from a squatted position. The average age of the patients with non-sporting related meniscal tears was 41. The authors felt that this age may reflect the degenerative changes in the meniscus, thereby requiring less force to create an injury. Smillie (1978) proposed that meniscus degeneration starts in the third decade of life. This degeneration reduces the elasticity of the meniscus, thereby increasing the susceptibility to injury. Drosos and Pozo deduced that degeneration may be the result of the repetitive micro-trauma and mechanical stresses of everyday life. These factors, in conjunction with the age-related disappearance of elastic fibers, may precede the development of many meniscal tears.

Previous research shows that there is a significant risk for meniscus damage associated with an increase in age and frequent and prolonged kneeling. [7, 10, 22, 23] Some meniscus tears can be repaired, while others will have to be removed in a meniscectomy. Although this procedure is necessary to ensure proper joint motion, it leaves the articular cartilage of the femur and tibia without a proper intermediate tissue. The weight bearing area of an intact meniscus

varies from 11 cm^2 at 90° flexion to 20 cm^2 at full extension. After meniscectomy the area ranges from 6 cm^2 to 12 cm^2, respectively. [13] This decreased area increases the peak local contact stresses transmitted to the articular cartilage by 65-235 %, causing degeneration. [24] Thus, meniscal injuries have been linked to the long-term development of knee osteoarthritis. [25 - 28]

1.3.3 Osteoarthritis

Osteoarthritis has been associated with a number of personal and activity-related risk factors. Personal risk factors include heredity, age, diabetes, smoking, and obesity. [3] Activity-related risk factors are trauma, sports activities, and occupation. [8, 17, 29, 30, 31] Within the occupational factors, a knee bending variable has been examined, including levels of knee bending, such as stooping, kneeling, crouching, or crawling. Of the 5,193 people surveyed, 315 were found to have radiographic osteoarthritis of the knee. Multiple linear regressions found knee bending demand of the job was associated with osteoarthritis of the knee (OR=0.32) amongst both men and women in the 55-64 years age group. The increased risk for osteoarthritis in those with physically demanding occupations was seen mostly in people 55 years and over (OR=2.45 in men, OR=3.49 in women). The authors concluded that the strong association with occupations in which knee bending is prominent suggests work activity may play a major causative role in osteoarthritis of the knee. [3]

Subsequent studies have suggested that the risk of developing knee osteoarthritis is increased by work involving prolonged knee bending and squatting. [3, 4, 17, 32] This is evident in the high prevalence of knee osteoarthritis among Asian populations who spend a lot of time performing floor activities. [17] The postures examined were squatting, side-knee bending, kneeling, and lotus position. Of these postures, squatting, lotus position, and side-knee bending were found to increase the risk of developing knee osteoarthritis.

2.0 MOTIVATION

Much attention has been given to the biomechanics of the knee joint during gait but the same attention has not been given to the knee joint while in kneeling, stooped, or squatted postures. Although there has been research on restricted postures, much of this research is aimed at the low back forces and causes of low back pain. There are few studies available on squatting and high flexion activities; however, no studies of kneeling on one knee or near 90° flexion were found.

2.1 PREVIOUS MODELLING OF KNEE FORCES AND MOMENTS

Dahlkvist et al. (1982) developed subject-specific 2-D models of the lower leg of six male subjects to determine the forces at the knee during squatting and rising from a deep squat. Anthropometric data and x-rays were used to create the model. External force reactions and points of application, lower leg configurations, and electromyographic data were measured. For three subjects, forces were calculated throughout going into a deep squat and then rising to a standing position. For the other three subjects rising from a deep squat were compared for a slow rise trial and a fast rise trial. Joint forces varied across subjects and during activities. Patellofemoral joint forces were shown to be the largest, with average maximums between 4.7 times bodyweight for slow ascent and 7.6 times bodyweight for fast descent.

Perry et al. (1975) performed a cadaver study to show significantly increased forces on the joint surfaces with flexion of greater than 30°. Forces in the quadriceps, patella, and tibia during simulated weight-bearing flexed knee stance were determined in a cadaver model. The specimen was instrumented to measure the quadriceps force, patellofemoral compression, and tibiofemoral loading. Flanged transducers were inserted into the tibia to measure the tibiofemoral joint stress. Quadriceps muscle action was simulated by a cable linked between the vastus intermedialus-rectus femoris to the intertrochanteric region of the femur. A ring tensiometer, aligned parallel to the femur, measured the forces in the cable as loads were applied to the femoral head. Compressive forces of the patella were also measured. The knee was set to six positions for measurement: 0°, 5°, 15°, 30°, 45°, and 60°. The quadriceps force necessary to stabilize the knee was found to be directly proportional to the femoral load and angle of flexion. At the 30° position, the required force was 210% body weight and at 60° the required force was 410% body weight. The tibiofemoral forces also increased in direct proportion to the load on the head of the femur when in full extension. When flexed, the tibiofemoral forces were a summation of the load on the femoral head and the quadriceps force. The patellar forces were found to be a function of quadriceps tension and dependent on the angle of flexion and the applied femoral load. [34]

Nagura et al. (2002) determined the forces during squatting activities using an inverse dynamics approach and found similar high contact forces. Subjects were separated into two groups, the ambulation group and the deep flexion group. Net moments and posterior forces were shown to be significantly higher in deep flexion than in walking or stair climbing. The net posterior force increased by 50% over walking and stair climbing. Net moments and inferior forces were significantly smaller in deep flexion than in walking or stair climbing. The authors concluded that the increase in extensor force during deep flexion increases the stress in the patellar tendon and joint contact forces. [35]

Sharrard (1965) examined the forces and pressures at the knee joint of a miner simulating a shoveling task while kneeling. He placed scales under the knees and toes of the miner. When the 189 lbs subject rested sitting on his heels, the weight on the left knee, right knee, and toes were 46 lbs, 56 lbs, and 84 lbs respectively. During the shoveling task, the weight on the knees and toes rose and declined rapidly. Results showed that the pressures can rise as much as 200 pounds per square inch while shoveling. At that time, the average miner shoveled once every 2.5 seconds. The pressures at the tibial tubercle, the interval between the tibial tubercle and the patella, the distal pole of the patella, and the body of the patella were also measured. These pressures were shown to vary throughout the shoveling task as well. Considerable variation was shown in the pressures and weight-bearing surfaces of the knee while kneeling and performing work. [9]

Previous biomechanical models of the knee used to evaluate deep flexion and squatting postures did not account for the contact between the thigh and the calf. [33, 34] Nagura et al. stated that neglecting this contact was a limitation of their study which may cause an overestimation of net forces and moment. Caruntu et al. (2003) created a model of the knee for

deep flexion which included the contact between the thigh and the calf. They reported a 700 N overestimation in quadriceps force when this contact was neglected. They also reported a 50% increase in medial collateral ligament forces when this contact was considered. [36] Zelle et al. (2007) measured the pressure distribution of thigh-calf contact for subjects squatting and kneeling with mean knee angles of 151.8 and 156.4 respectively. Results showed the resultant contact force to be >30% body weight and located within 17 cm of the epicondylar axis. [5] Thigh-calf contact has been shown to be significant, and neglecting these parameters may result in overestimation of joint forces and moments. For these reasons the contact force between the thigh and the calf was not neglected from this computational knee model.

In summary previous research on knee biomechanics in restricted postures have failed to examine kneeling near 90° flexion and kneeling on one knee, which may be commonly utilized when performing work. Research on higher flexion postures such as kneeling near full flexion and squatting did not include thigh-calf or heel-gluteus contact and may result in the overestimation of joint forces and moments. In this research a computational model was develop to determine the net dynamic forces and moment imposed on the knee during static kneeling postures. This model may be applied to other postures in the future and accounts for the contact between the thigh and the calf as well as between the heel and the gluteal muscles which may occur when kneeling in high flexion.

2.2 SPECIFIC AIMS AND SIGNIFICANCE

2.2.1 Specific Aim #1

Develop algorithms and a 3-D computational model to calculate the net dynamic forces and moments at the knee joint from motion capture and force plate data

To date, there has not been an analysis of the forces and moments at the knee during kneeling. Previous research has determined the net forces and moments at the knee joint for squatting and end range flexion. [33 -36] The role of this study was to develop a computational model that may be used to determine the net forces and moments of the knee during not only squatting and deep flexion, but also for kneeling near 90° flexion and kneeling on one knee. The use of one computational model to analyze different postures will allow for better comparisons and interpretation of these forces and moments. Also, unlike traditional models based on inverse dynamics, this model accounts for the contact force between the thigh and calf, which has been determined to be >30% body weight. [5] At this level of force, this contact may be sufficient to have a considerable effect on the forces, moments, and stresses in knee structures. This model also accounts for the contact between the heel and the gluteal muscles which occurs in some people when kneeling and sitting on their heels.

2.2.2 Specific Aim #2

Apply the developed model to data collected from a minimum of one subject.

The effect of protective equipment (i.e. knee pads) on knee forces and moments has not been investigated. In this study the subject was evaluated with and without knee pads. The forces were not expected to change significantly due to the knee pads however, the knee pads were expected to change the location of the center of pressure for the force at the knee-ground interface, thereby affecting the moments at the knee. Force plate, motion capture, and pressure data were analyzed via the developed model for two subjects. This model will be used in the future on a larger dataset currently being collected. The resulting forces and moments will add to the knowledge on kneeling biomechanics. In addition, these forces and moments will be utilized in the finite element model of the knee currently being developed.

2.2.3 Specific Aim #3

A sensitivity analysis for the input variables (anthropometric variables, joint center location estimation, ground reaction forces, thigh-calf contact force, and heel-gluteal contact force) will be implemented.

Numerous factors contribute to the forces and moments at the knee joint while kneeling. A sensitivity analysis was performed to determine which variables contribute the most to the forces and the moments at the knee. This analysis was also useful in determining which parameters introduce the largest sources of error in the model.

2.2.4 Future Significance

The forces and moments determined using this computational model will be inputs to a finite element model (FEM) of the knee being developed. This FEM will be used to evaluate the stresses and strains in tissues while kneeling, crawling, and stooping. Results of the FEM will provide a better understanding of the internal biomechanics of the knee structures while in restricted postures. These results will be used to provide interventions, such as a novel knee pad design, in hopes of reducing the prevalence and severity of occupational knee injuries in low-seam coal miners.

3.0 RESEARCH DESIGN AND METHODS

Motion analysis and force data were collected to track body positions and ground reaction forces for simulated postures. This data was used to determine the segment positions, segments lengths, and ground reaction forces. Pressure data were also collected to determine the magnitude of the force transmitted from the thigh to the calf and from the heel to the gluteal muscles when kneeling. These parameters were inputs into the computation model, allowing the estimation of knee forces, moments, and joint angles.

3.1 EQUIPMENT

3.1.1 Laboratory Equipment

Motion data is captured using eleven Infrared cameras (Eagle, Motion Analysis Corporation, Santa Rose, California, USA) which track the motion of ½" reflective markers. The cameras are arranged around the room such that all markers are visible during testing. Motion data was collected at 60 Hz.

Two force platforms (Model OR6-5, Advanced Mechanical Technology, Inc., Newton, Massachusetts, USA) were used to measure the reaction forces at the ground-knee, ground-foot, or ground-kneepad interface. The force platforms were aligned in parallel and were level with the floor. Force data was collected at 1020 Hz.

A clinical seating pressure assessment system (ClinSeat®, Tekscan Inc., South Boston, Massachusetts, USA) was used to measure the contact between the thigh and calf and the heel and gluteal muscles. This 19.2 in x 16.8 in pressure sensor uses resistive technology to measure the pressure between surfaces. The spatial resolution is 1 sensel/cm^2 with a pressure range of 0-30 PSI. The supplied software (Advanced ClinSeat, Tekscan Inc., South Boston, Massachusetts, USA) generated pressure maps, total pressure, total force, and center of pressure. Total force and center of pressure locations from the supplied software were used in the computational model.

3.1.2 Computational Model

The computational model was developed in MATLAB® (The Mathworks Inc., Natick, MA) on a personal computer. It is based on an inverse dynamics method [37] which uses measured ground reaction forces and anthropometric measurements to determine the net external forces and moments at the right knee joint. In this linear model the upper leg (femur) and the lower leg (tibia, fibula, and foot) are modeled as rigid bodies attached via a pin joint with three rotational degrees of freedom. The global reference frame was oriented such that when the subject was standing in standard anatomical position, the x-axis was in the medial/lateral direction, the y-axis was in the anterior/posterior direction, and the z-axis was in the superior/inferior direction. The origin of this system was on the laboratory floor at the upper left corner of the first force plate.

3.1.2.1 Model Assumptions

The developed computational model is based on several assumptions.

- *The knee is assumed to be a frictionless pin-joint.* This allows all forces to pass directly through the joint center.
- *Segments are assumed to be rigid with mass concentrated at the center of mass locations.* This allows one center of mass to represent the weight of the segment.
- *Linear relationship between external forces and moments applied to the knee.* This allows a planar model to be used to determine the external forces and moments applied to the knee.
- *The relative movement of pelvic bones is negligible.* This allows approximation of the hip joint center from palpable pelvic landmarks.
- *Thickness of subcutaneous tissue between bone and skin is minimal.* This allows the assumptions that markers placed on palpable landmarks are directly on that landmark.
- *The measured thigh-calf and heel-gluteus contact forces are concentrated at the measured center of pressure location.* This allows the contact forces to be represented as a single resultant force, opposed to a pressure distribution.
- *Affect of patellar tendon and tibial tubercle on forces externally applied to the tibia is negligible.* This assumption allows ground contact forces measured at the ground-knee or ground-kneepad interface to be assumed to act at some distance away from the knee joint center and not be affected by the patellar tendon or tibial tubercle.

3.2 SUBJECT TESTING

3.2.1 Thigh-Calf and Heel-Gluteus Contact Measurements

Thigh-calf and heel-gluteus contact forces ($F_{t/c}$ and $F_{h/g}$) were measured prior to motion and force data collection. The subject was instructed to kneel near 90° flexion and the pressure sensor was placed on their lower leg. The subject was then instructed to kneel into full flexion while pressure data was collected for a period of 5 seconds. The distance from the top of the sensor to the lateral epicondyle was measured and recorded while data was collected. This was repeated with the subject squatting.

3.2.2 Subject Instrumentation

Each subject was fitted with 41 reflective markers using a modified version of the Cleveland Clinic Foundation's marker set, Figure 2. The marker included one segment marker and a three marker cluster of the thighs and shanks. This marker set was chosen to be compatible with SIMM for use in a future study. The subject was instructed to perform a standing T-pose with their right foot making contact with force plate 2 and their left foot off of the force plates. Data was collected for 5 seconds. This data was used to create the anatomical coordinate system for the thigh and shank.

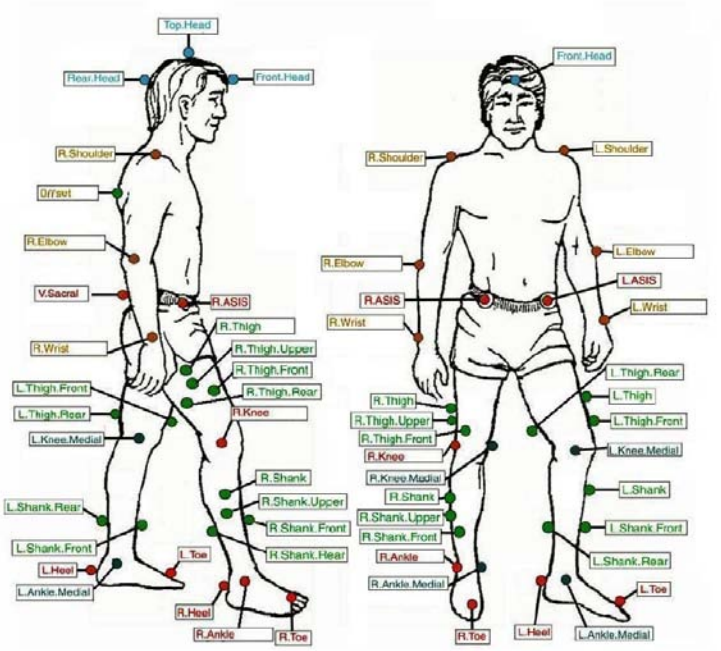

Figure 2: Anatomical marker set

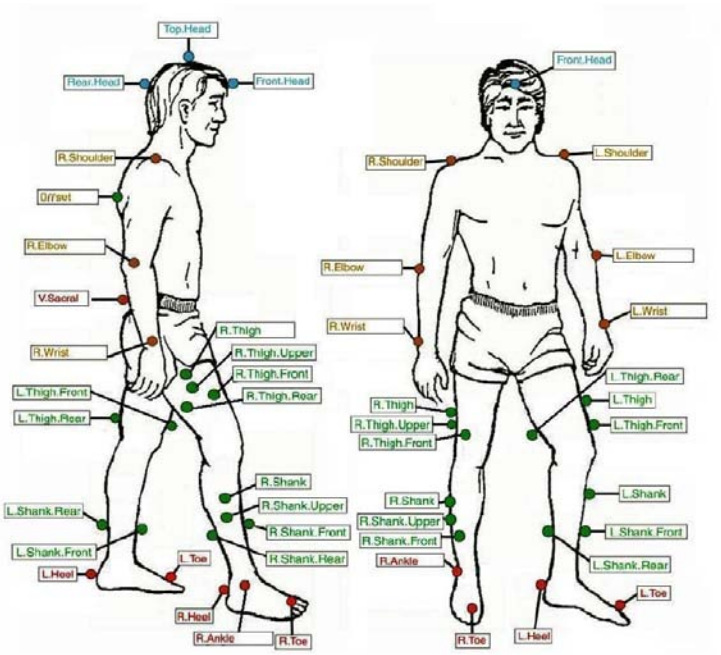

Figure 3: Measured marker set

Following recording of the standing T-pose, eight markers were removed due to their high risk for falling off or becoming covered (i.e. they are virtual markers which were reconstructed during data processing). This yielded the measured marker set shown in Figure 3. The subject was instructed to perform another standing T-pose as well as a range of motion. During the range of motion, the subject went through a series of motions with a laboratory assistant. They began in a standing T-pose then performed lateral bending, twisting at waist, raising knees up to chest, squatting, and knee flexion/extension, crossing arms, rotating head then dropped down into a kneeling posture. In this kneeling posture the subject performed lateral bending, twisting at waist, kneeling down into full flexion, kneeling on left knee, kneeling on right knee, ankle rotations, kneeling on all fours, and ended in a standing T-pose. The range of motion data was then post-processed and used to extend the motion capture template.

3.2.3 Experimental Data Collection

Once the template was extended, experimental data collection began. A mesh roof in the laboratory was lowered to 48", simulating a restricted working height. The subject was instructed to perform a static trial of each posture for 10 seconds. The postures studied were kneeling near 90° flexion, kneeling on the right knee, kneeling near full flexion, and squatting. Subjects were not given specific instructions on these postures. A poster in the laboratory showed schematics of the postures studied, Figure 4. Subjects were instructed to simulate the postures shown in the schematics. They were not given specific instructions on kneeling postures as to not affect their normal kneeling postures. They were, however given instructions on where to place their knees and feet when kneeling. When testing the kneeling near 90° flexion, kneeling on right knee, and kneeling near full flexion, subjects were instructed to kneel

with their right knee on force plate 2 and their right foot on force plate 1. Their left side was to remain off of the force plates. When testing the squatting posture, subjects were instructed to kneel with their right foot on force plate 2 and their left foot off of the force plates. At the start of testing, each subject was provided a new pair of orange articulating knee pads commonly worn by underground coal miners, Figure 5. The subject performed each posture with and without knee pads for a total of eight trials. Motion data was low-pass filtered using a 4th order Butterworth filter at 15 Hz to smooth instrumental errors.

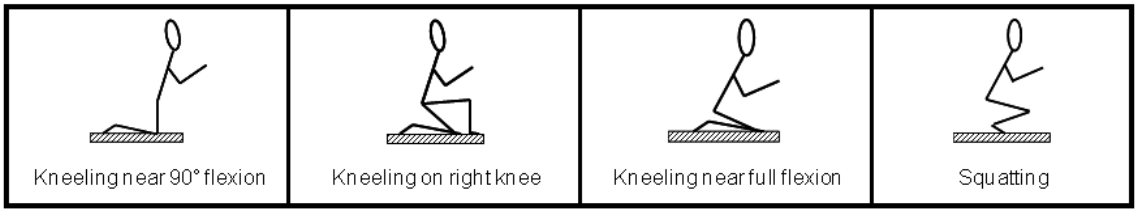

Figure 4: Postures assumed by subjects during testing

Figure 5: Articulating kneepads commonly worn by low-seam coal miners

3.3 DATA ANALYSIS

Data was analyzed for a 5 five second period of the trial after the subject appeared to have reached a balanced posture and showed minimal instability. This portion of the static trial was used to determine the forces, moments, and joint angles.

3.3.1 Construction of Coordinate Systems

For each segment, an anatomical and measured coordinate system was created from the motion capture data. The anatomical system was created from the anatomical standing T-pose and allowed the location of anatomical landmarks to be linked to the global reference frame. It was also used to determine the location of the ankle joint center (AJC), knee joint center (KJC), and hip joint center (HJC) as well as the location of the lower leg center of mass. A measured coordinate system was created from the anatomical standing T-pose as well as from each static trial and was used to link the testing markers to the locations of the markers that were removed.

The anatomical coordinate system of the thigh (ATCS) was created using the left and right anterior superior iliac spine (L.ASIS & R.ASIS), knee, and thigh markers.

$$r_1 = \frac{knee\ lateral\ - knee\ medial}{\left| knee\, lateral - knee\, medial \right|} \qquad x-axis$$

$$r_2 = \frac{HJC\ - KJC}{\left| HJC - KJC \right|}$$

$$r_3 = r_2 \times r_1 \qquad y-axis$$

$$r_4 = r_1 \times r_3 \qquad z-axis$$

The KJC was assumed to be midway between the medial and lateral epicondyles of the femur, measured by the medial and lateral knee markers. The location of the HJC was approximated using regression equations proposed by Bell et al. (1990) and adapted to fit the global reference frame of the laboratory. [38] (Figure 6)

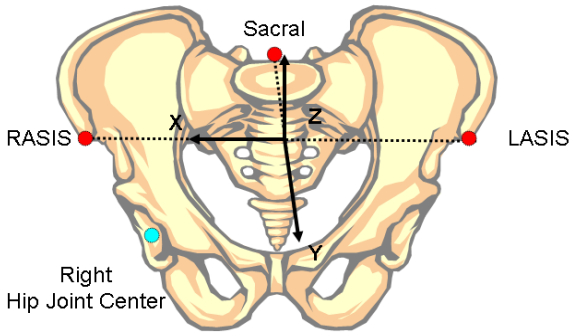

Figure 6: Pelvis coordinate system highlighting the location of the right hip joint center

$$Origin = \frac{LASIS + RASIS}{2}$$

$$PW = \left| RASIS_x - LASIS_x \right|$$

$$HJC = \begin{bmatrix} Origin + .36 * PW \\ Origin - .19 * PW \\ Origin - .3 * PW \end{bmatrix}$$

The transformation matrix from the global reference frame to the anatomical thigh coordinate system (T_{TGA}) was created from the unit direction vectors of the ATCS.

$$T_{TGA} = \begin{bmatrix} 1 & 0 & 0 & 0 \\ \begin{bmatrix} \\ HJC \\ \\ \end{bmatrix} & \begin{bmatrix} \\ r_1 \\ \\ \end{bmatrix} & \begin{bmatrix} \\ r_3 \\ \\ \end{bmatrix} & \begin{bmatrix} \\ r_4 \\ \\ \end{bmatrix} \end{bmatrix}$$

The anatomical coordinate system of the shank (ASCS) was determined using the knee, ankle, and shank markers. The AJC was assumed to be midway between the medial and lateral malleoli, measured by the medial and lateral ankle markers. The transformation matrix from the GCS to the ASCS (T_{SGA}) was created from the unit direction vectors of the ASCS.

$$r_1 = \frac{knee\ lateral - knee\ medial}{\left| knee\ lateral - knee\ medial \right|}$$

$$r_2 = \frac{KJC - AJC}{\left| KJC - AJC \right|} \qquad z-axis$$

$$r_3 = r_1 \times r_2 \qquad y-axis$$

$$r_4 = r_3 \times r_1 \qquad x-axis$$

$$T_{SGA} = \begin{bmatrix} 1 & 0 & 0 & 0 \\ \begin{bmatrix} \\ KJC \\ \\ \end{bmatrix} & \begin{bmatrix} \\ r_4 \\ \\ \end{bmatrix} & \begin{bmatrix} \\ r_3 \\ \\ \end{bmatrix} & \begin{bmatrix} \\ r_1 \\ \\ \end{bmatrix} \end{bmatrix}$$

The ATCS and ASCS were oriented such that when standing the systems aligned with the GCS and the positive x-axis is in the lateral direction of the right leg, the positive z-axis is in the proximal direction, and the positive y-axis is in the anterior direction. (Figure 7)

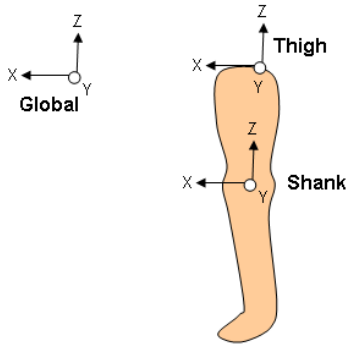

Figure 7: Orientation of the ATCS and ASCS

A measured coordinate system (MCS) was created for the thigh and the shank using the marker clusters on the segments. The measured coordinate system of the thigh (MTCS) was created from the thigh, thigh front, and thigh rear markers. The transformation matrix from the GCS to the MTCS (T_{TGM}) was also created with the right thigh front marker as its origin.

$$r_1 = \frac{thigh - thigh\ front}{|thigh - thigh\ front|} \qquad z-axis$$

$$r_2 = \frac{thigh\ front - thigh\ rear}{|thigh\ front - thigh\ rear|}$$

$$r_3 = r_2 \times r_1 \qquad x-axis$$

$$r_4 = r_1 \times r_3 \qquad y-axis$$

$$T_{TGM} = \begin{bmatrix} 1 & 0 & 0 & 0 \\ thigh\ front & r_3 & r_4 & r_1 \end{bmatrix}$$

The measured coordinate system of the shank (MSCS) was created from the shank, shank front, and shank rear markers. The transformation matrix from the MSCS to the GCS (T_{SGM}) was created with the right shank front marker as its origin.

$$r_1 = \frac{shank - shank\ \ front}{\left|shank - shank\ \ front\right|} \qquad z - axis$$

$$r_2 = \frac{shank\ \ front - shank\ rear}{\left|shank\ \ front - shank\ rear\right|}$$

$$r_3 = r_2 \times r_1 \qquad x - axis$$

$$r_4 = r_1 \times r_3 \qquad y - axis$$

$$T_{SGM} = \begin{bmatrix} 1 & 0 & 0 & 0 \\ shank\ \ front & r_3 & r_4 & r_1 \end{bmatrix}$$

To determine measured marker locations in the ATCS and ASCS, T_{TMA} and T_{SMA} were created respectively.

$$T_{TMA} = \left[T_{TGM}\right]^{-1}\left[T_{TGA}\right]$$

$$T_{SMA} = \left[T_{SGM}\right]^{-1}\left[T_{SGA}\right]$$

3.3.2 Joint Angle Estimation

Joint angles were determined for each trial using Euler Angle Decomposition. The largest joint rotations occurred about the medial/lateral x-axis (α – extension/flexion) followed by the posterior/anterior y-axis (β - varus/valgus), and the distal/proximal z-axis (γ - internal/external rotation), yielding an Euler order of Xy'z''. The transformation matrix from the anatomical thigh to the anatomical shank coordinates T_{ST} was created to determine the rotation matrix, R_{ST}. This matrix was used to determine the Euler angles. Therefore, motion of the thigh was in respect to the shank.

$$T_{SGA} = [T_{SGM}] * [T_{SMA}]$$

$$T_{TGA} = [T_{TGM}] * [T_{TMA}]$$

$$T_{ST} = [T_{SGA}]^{-1} * [T_{TGA}]$$

$$R_{ST} = \begin{bmatrix} 1 & 0 & 0 \\ 0 & \cos(\alpha) & -\sin(\alpha) \\ 0 & \sin(\alpha) & \cos(\alpha) \end{bmatrix} * \begin{bmatrix} \cos(\beta) & 0 & \sin(\beta) \\ 0 & 1 & 0 \\ -\sin(\beta) & 0 & \cos(\beta) \end{bmatrix} * \begin{bmatrix} \cos(\gamma) & -\sin(\gamma) & 0 \\ \sin(\gamma) & \cos(\gamma) & 0 \\ 0 & 0 & 1 \end{bmatrix}$$

$$R_{ST} = \begin{bmatrix} \cos(\beta)\cos(\gamma) & -\cos(\beta)\sin(\gamma) & \sin(\beta) \\ \sin(\gamma)\cos(\alpha) + \sin(\beta)\cos(\gamma)\sin(\alpha) & \cos(\gamma)\cos(\alpha) - \sin(\beta)\sin(\alpha)\sin(\gamma) & -\cos(\beta)\sin(\alpha) \\ \sin(\gamma)\sin(\alpha) - \sin(\beta)\cos(\gamma)\cos(\alpha) & \cos(\gamma)\sin(\alpha) + \sin(\beta)\sin(\alpha)\cos(\gamma) & \cos(\beta)\cos(\alpha) \end{bmatrix}$$

$$\gamma = \tan^{-1}\left(\frac{-\left(-\cos(\beta)\sin(\gamma)\right)}{\cos(\beta)\cos(\gamma)}\right) = \tan^{-1}\left(\frac{-R_{ST_{1,2}}}{R_{ST_{1,1}}}\right)$$

$$\alpha = \tan^{-1}\left(\frac{-\left(-\cos(\beta)\sin(\alpha)\right)}{\cos(\beta)\cos(\alpha)}\right) = \tan^{-1}\left(\frac{-R_{ST_{2,3}}}{R_{ST_{3,3}}}\right)$$

$$\beta = \tan^{-1}\left(\frac{\cos(\gamma)\sin(\beta)}{\cos(\beta)\cos(\gamma)}\right) = \tan^{-1}\left(\frac{\cos(\gamma)R_{ST_{1,3}}}{R_{ST_{1,1}}}\right)$$

3.3.3 Joint Forces and Moments

Ground reaction forces, segment weight, $F_{t/c}$, and $F_{h/g}$ were inputs into the computational model. External force diagrams for kneeling near full flexion with respect to the GCS and the ASCS are shown in Figure 8 and Figure 9. The center of mass location and weight of the shank+foot were determined using equations from Clauser et al., 1969 which were adjusted to use the knee joint center and ankle joint center in this model. [40] The reaction forces and moments were assumed to act in the positive directions.

Squatting and kneeling creates a contact force between the thigh and the calf. Kneeling near full flexion also creates this contact, and in some subjects there is additional contact between the heel and the gluteal muscles. $F_{t/c}$ and $F_{h/g}$ were modeled as resultant forces whose line of action was in the anterior direction of the shank. The locations of these forces were determined from the center of pressure locations on the pressure sensor. Forces at the foot (F_1), forces at the knee (F_2) and the weight of the lower leg were measured with respect to the GCS. (Figure 8) Thigh-calf and heel-gluteus contact forces were measured with respect to the ASCS.

Figure 9 shows the orientation of the forces and moments as presented in this research, with respect to the ASCS. External force diagrams for all postures are shown in Figure 10.

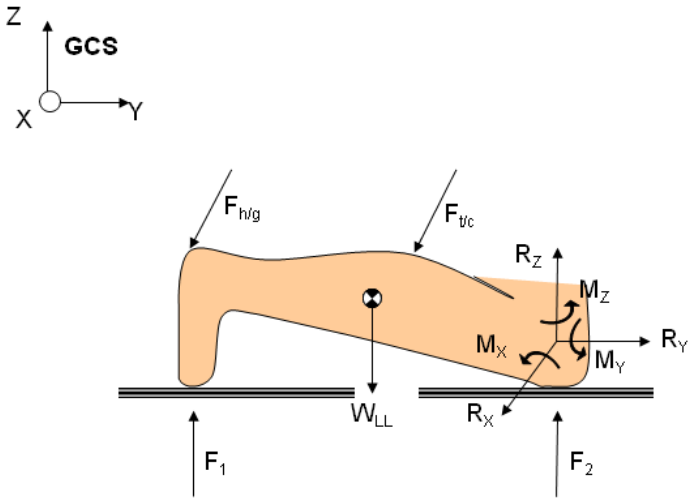

Figure 8: Diagram of external shank forces and reaction forces and moments for kneeling near full flexion with respect to the GCS

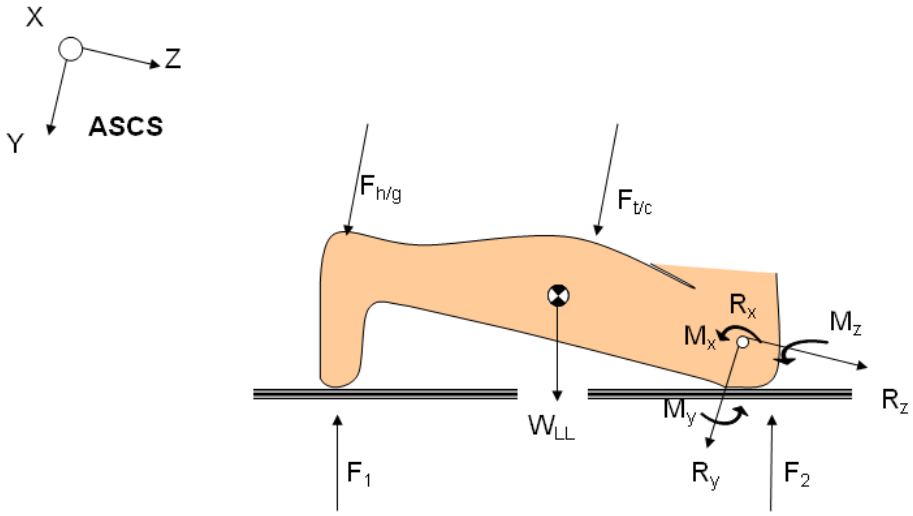

Figure 9: Diagram of external shank forces and reaction forces and moments for kneeling near full flexion with respect to the ASCS

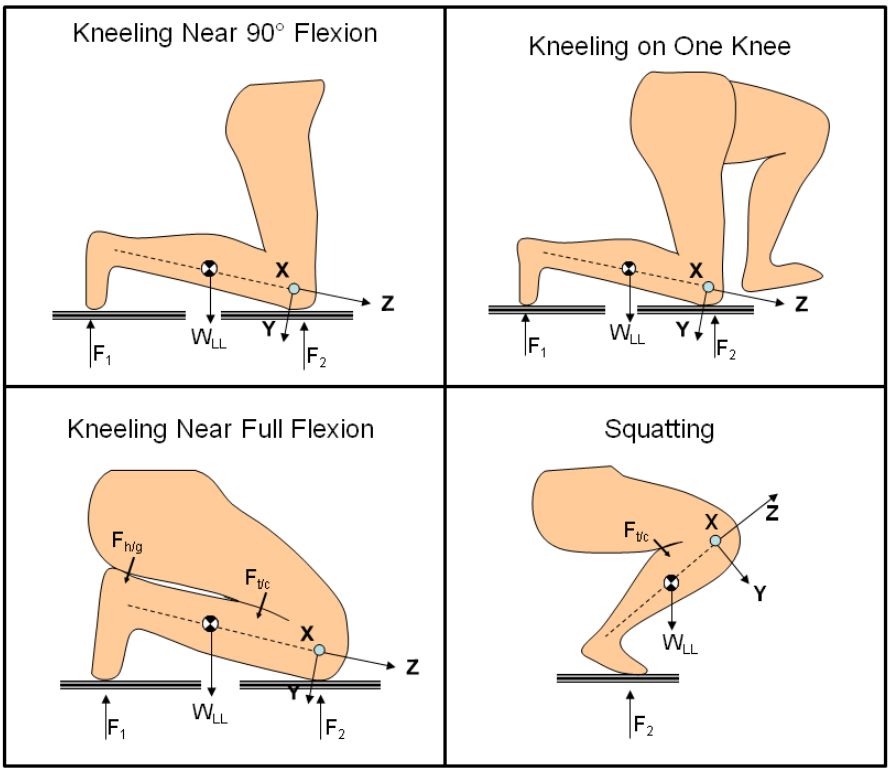

Figure 10: External force diagrams with respect to the anatomical shank coordinate system

Joint equilibrium was assumed, therefore the sum of all forces and moments at the knee were calculated and summed to equal zero. The sum of the external forces in the x, y, and z directions were all summed to zero to determine the reaction force, R, necessary to stabilize the knee due to the application of the net external forces (F_{knee}).

$$\sum F_x = 0$$
$$F_{1x} + F_{2x} + R_x = 0$$
$$R_x = -F_{1x} - F_{2x}$$

$$\sum F_y = 0$$
$$F_{1y} + F_{2y} + R_y = 0$$
$$R_y = -F_{1y} - F_{2y}$$

$$\sum F_z = 0$$
$$F_{1z} + F_{2z} + R_z - W_{LL} - F_{t/c} - F_{h/g} = 0$$
$$R_z = W_{LL} - F_{1x} - F_{2x} - F_{t/c} - F_{h/g}$$

$$F_{knee} = -(R_x + R_y + R_z)$$

The sum of the external moments at the knee joint in the x, y, and, z directions were also summed to equal zero. The net external knee moment applied to the knee joint (M_{knee}) was also determined.

$$M_{F1} = \begin{bmatrix} KJC_{1x} - COP_{1x} & KJC_y - COP_{1y} & KJC_z - COP_{1z} \end{bmatrix} \times \begin{bmatrix} F_{1x} & F_{1y} & F_{1z} \end{bmatrix}$$
$$M_{F2} = \begin{bmatrix} KJC_x - COP_{2x} & KJC_y - COP_{2y} & KJC_z - COP_{2z} \end{bmatrix} \times \begin{bmatrix} F_{2x} & F_{2y} & F_{2z} \end{bmatrix}$$

$$M_{LL} = \begin{bmatrix} KJC_x - COM_{LLx} & KJC_y - COM_{LLy} & KJC_z - COM_{LLz} \end{bmatrix} \times \begin{bmatrix} 0 & 0 & -W_{LL} \end{bmatrix}$$

$$M_{t/c} = \begin{bmatrix} KJC_x - COP_{Ft/cx} & KJC_y - COP_{Ft/c_y} & KJC_z - COP_{Ft/c_z} \end{bmatrix} \times \begin{bmatrix} 0 & 0 & -F_{t/c} \end{bmatrix}$$
$$M_{h/g} = \begin{bmatrix} KJC_x - COP_{Fh/g_x} & KJC_y - COP_{Fh/g_y} & KJC_z - COP_{Fh/g_z} \end{bmatrix} \times \begin{bmatrix} 0 & 0 & -F_{h/g} \end{bmatrix}$$

$$\sum M_{KJC} = 0$$
$$M_{KJC} + M_{t/c} + M_{h/g} + M_{F2} + M_{F1} + M_{LL} = 0$$
$$M_{KJC} = -(M_{t/c} + M_{h/g} + M_{F2} + M_{F1} + M_{\mathrm{LL}})$$

$$M_{knee} = -M_{KJC} = M_{t/c} + M_{h/g} + M_{F2} + M_{F1} + M_{\mathrm{LL}}$$

4.0 RESULTS

Data from two subjects were analyzed using the developed computation model. Subject 1 was a 1.8 m, 675 N, 19 year old male. Subject 2 was a 1.56 m, 720 N, 59 year old female. Neither subject had a history of knee injuries or pathologies. All forces and moments presented are in reference to the anatomical shank coordinate system.

4.1 THIGH-CALF AND HEEL-GLUTEUS CONTACT FORCES

4.1.1 Near Full Flexion

The mean $F_{t/c}$ in the kneeling near full flexion posture for subjects 1 and 2 were 127.5 N and 164 N, respectively. The centers of pressure were 0.14 m, and 0.17 m along the long axis of the tibia from the medial epicondyle of the femur. Pressure distributions, showing the centers of pressure for this posture are shown in Figure 11. Subject 2's posture did not cause any contact between the heel and gluteal muscles. Subject 1 had a mean $F_{h/g}$ of 56.1 N with a center of pressure 0.43 m along the long axis of the tibia from the medial epicondyles of the femur. This pressure distribution is shown in Figure 12.

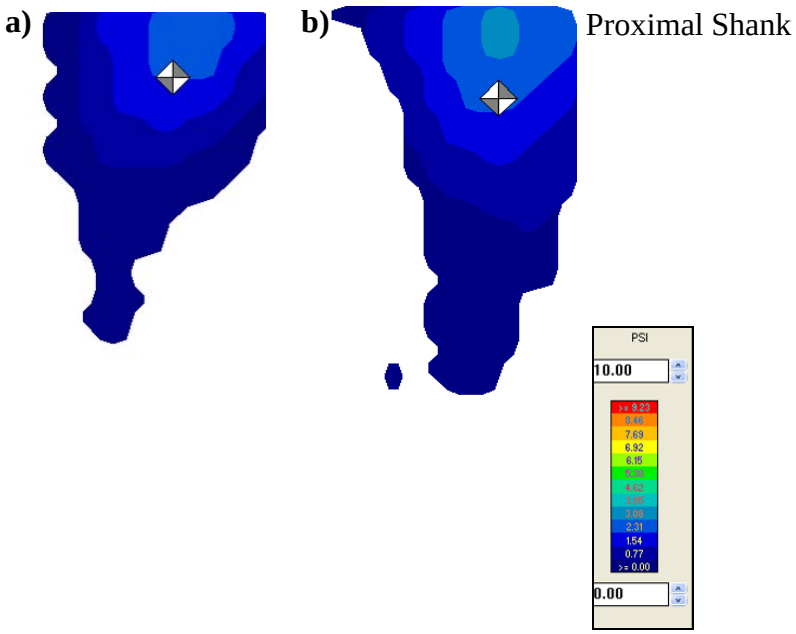

Figure 11: Thigh-calf contact pressure distributions for kneeling near full flexion

a) Subject 1 b) Subject 2

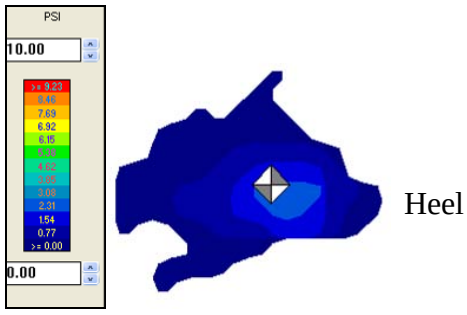

Figure 12: Heel-gluteus pressure distribution for kneeling near full flexion, Subject 1

4.1.2 Squat

The mean $F_{t/c}$ in the squatting posture for subjects 1 and 2 were 173 N and 195 N, respectively. The centers of pressure were located 0.15 m, and 0.14 m along the long axis of the tibia from the medial epicondyle of the femur. Pressure distributions, showing the centers of pressure for this posture are shown in Figure 13.

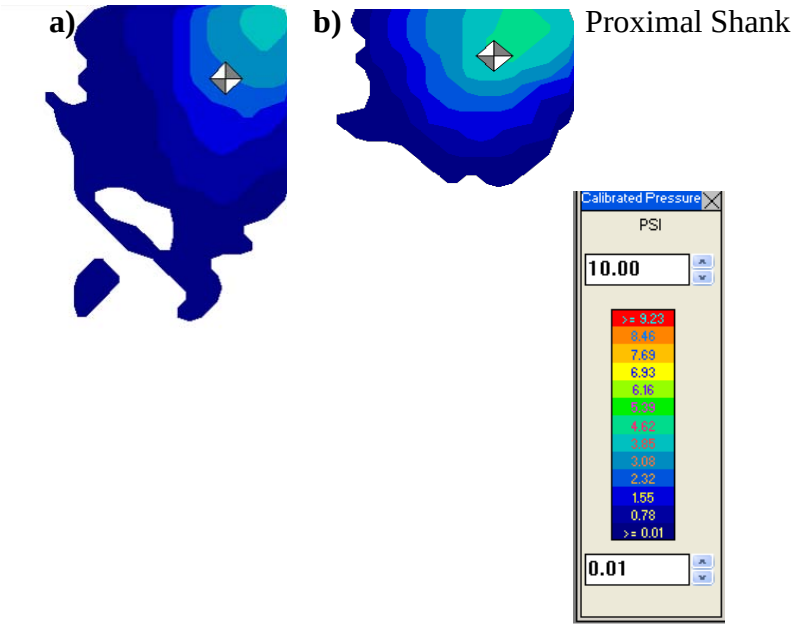

Figure 13: Thigh-calf contact pressure distributions for squat

a) Subject 1 b) Subject 2

4.2 KNEE ANGLES

Mean varus/valgus, internal/external rotation, and included knee angles for Subjects 1 and 2 are shown in Table 1 and Table 2, respectively. Standard deviations across 5 second portions of the trials are shown in parentheses. The angles varied over time with standard deviations ranging from .22-1.44° for the included angles, .36-8.69° for varus/valgus, and .25-1.98° for int/ext rotation. Both subjects had very small standard deviations in the included joint angles over time. Varus/valgus deviations were the largest for both subjects. Subject 1 ranged from 15° varus to 15° valgus when wearing kneepads and kneeling near 90° flexion. This 30° range in angles caused a standard deviation of 8.55°. Subject 2 ranged from 3° varus to 3° valgus when wearing kneepads and kneeling on one knee, creating a standard deviation of 2.1°. A typical time series plot of the joint angles is shown in Figure 14.

Table 1: Average knee angle (degrees), Subject 1

Subject 1						
	With Kneepads			Without Kneepads		
	Included	+ Valgus - Varus	+ Int rot - Ext rot	Included	+ Valgus - Varus	+ Int rot - Ext rot
Near 90° Flexion	83.1 (1.35)	0.35 (8.55)	-4.7 (0.73)	82.7 (.25)	-7.3 (3.0)	-7.3 (0.28)
One Knee	80.2 (0.39)	-1.0 (3.41)	-14.0 (0.42)	75.9 (0.30)	8.7 (3.45)	-10 (0.44)
Near Full Flexion	23.0 (0.21)	1.2 (0.29)	6.5 (0.47)	23.0 (0.16)	2.1 (0.60	5.6 (0.32)
Squat	24.0 (0.78)	0.9 (2.47)	5.6 (1.55)	22.2 0.43)	1.3 (1.87)	5.7 (1.07)
Standing				173.6 (.57)	-2.6 (.22)	-.78 (.07)

Table 2: Average knee angles (degrees), Subject 2

Subject 2						
	With Kneepads			Without Kneepads		
	Included	+ Valgus - Varus	+ Int rot - Ext rot	Included	+ Valgus - Varus	+ Int rot - Ext rot
Near 90° Flexion	84.9 (.40)	-.81 (.51)	5.28 (.31)	38.9 (.5)	-9.1 (1)	5.9 (.27)
One Knee	40.6 (.48)	.40 (2.1)	4.7 (1.4)	35.8 (.32)	-4 (1.7)	.28 (.69)
Near Full Flexion	33.7 (.25)	-.58 (.69)	13.9 (.25)	31.9 (.1)	1.9 (1.6)	1.9 (.31)
Squat	36.3 (.46)	-.09 (.26)	12.7 (.55)	37.9 (.47)	-.63 (1.35)	7.5 (.77)
Standing				179.1 (.34)	-2.35 (.14)	-.05 (.02)

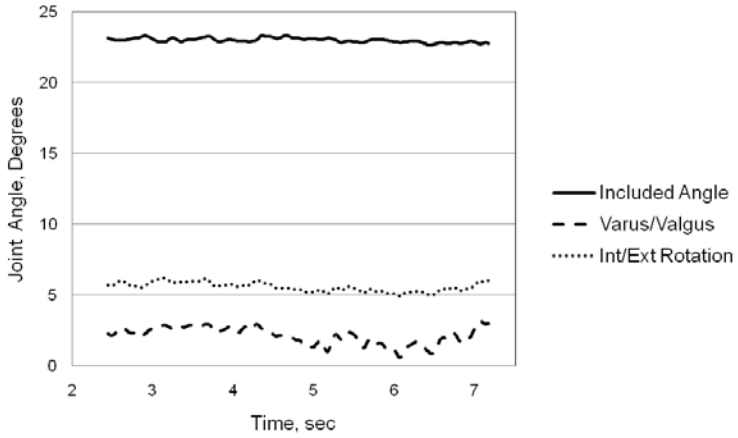

Figure 14: Joint angles for Subject 1 kneeling near full flexion without kneepads

4.3 KNEE FORCES

All forces are with respect to the anatomical shank coordinate system and normalized to body weight, by dividing the force in N, by the body weight in N, and multiplying by 100% yielding values in percentage of body weight (%BW). Average net forces for Subjects 1 and 2 are shown in Table 3 and Table 4, respectively. The largest lateral forces were found in Subject 1 when kneeling on one knee and the largest medial forces were shown in Subject 2 when squatting without kneepads. The largest posterior forces were shown when kneeling on one knee in both subjects. The largest proximal forces occurred in Subject 1 when squatting and in Subject 2 when kneeling on one knee. Time series of the net forces for Subject 1 kneeling near full flexion without kneepads are shown in Figure 15.

Table 3: Average net external forces normalized by body weight, Subject 1

Subject 1						
	With Kneepads, % BW			Without Kneepads, % BW		
	+ Lateral - Medial	+ Anterior - Posterior	+ Proximal - Distal	+ Lateral - Medial	+ Anterior - Posterior	+ Proximal - Distal
Near 90° Flexion	6.00 (.74)	-43.08 (.78)	-6.50 (.74)	8.61 (.34)	-41.29 (.41)	-6.21 (.20)
One Knee	16.70 (.87)	-74.62 (1.07)	-13.58 (.57)	7.33 (.41)	-67.80 (1.61)	-13.63 (.33)
Near Full Flexion	5.95 (.30)	-16.57 (.78)	-8.23 (.26)	5.61 (.56)	-17.67 (.69)	-7.65 (.68)
Squat	5.70 (.38)	-13.23 (1.27)	27.53 (1.10)	2.94 (.78)	-14.86 (1.54)	27.86 (.78)
Standing				.57 (.14)	-11.58 (.62)	39.89 (1.51)

Table 4: Average net external forces normalized by body weight, Subject 2

Subject 2						
	With Kneepads			Without Kneepads		
	+ Lateral - Medial	+ Anterior - Posterior	+ Proximal - Distal	+ Lateral - Medial	+ Anterior - Posterior	+ Proximal - Distal
Near 90° Flexion	-1.81 (.39)	-45.80 (.29)	-8.30 (.28)	-8.18 (.21)	-43.79 (.31)	-23.06 (.18)
One Knee	-3.07 (.92)	-53.40 (.51)	-12.75 (.51)	-8.31 (.72)	-55.88 (.60)	-28.99 (.37)
Near Full Flexion	-4.49 (.16)	-19.93 (.28)	-16.12 (.19)	-6.24 (.29)	-22.22 (.19)	-18.85 (.26)
Squat	-6.74 (.61)	-16.56 (.79)	15.14 (.73)	-10.52 (.46)	-11.42 (.80)	16.86 (.41)
Standing				.66 (.08)	-5.12 (.29)	42.20 (.69)

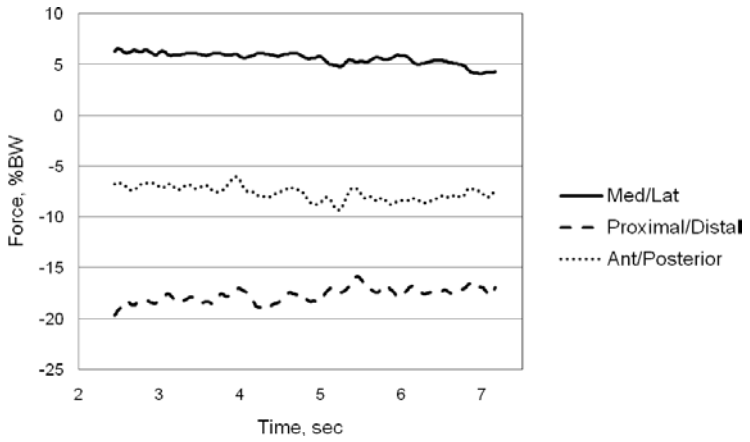

Figure 15: Net external forces normalized by body weight for Subject 1 kneeling near full flexion without kneepads

4.4 KNEE MOMENTS

All moments are in respect to the anatomical shank coordinate system and normalized to a percentage of the body weight*height to reduce the differences in moments due to gender. [41] The body weight in Newtons was multiplied by the height in meters, yielding a value in Nm. All moments were divided by this body weight*ht value, yielding moments with units in %BW*Ht. Average net moments for each posture with and without kneepads are shown in Table 5 and Table 6. All sagittal moments imposed on the knee due to static kneeling were flexion moments. Adduction moments occurred in Subject 1 for all postures. Adduction moments were created in Subject 2 when kneeling near 90° flexion and kneeling on one knee with kneepads. Abduction moments were shown in all postures without kneepads and when kneeling near full flexion and squatting with kneepads. Subject 1 showed external rotation moments when kneeling near full flexion without kneepads and when squatting. Kneeling near 90° flexion, kneeling on one knee, and kneeling near full flexion resulted in internal rotation moments. Subject 2 showed internal rotation moments for all postures. Time series showing the sagittal moment contributions for Subject 1 kneeling near full flexion without kneepads are shown in Figure 16.

Table 5: Average net external knee moments normalized by Body weight*Height, Subject 1

Subject 1						
	With Kneepads			Without Kneepads		
	Flexion	Adduction	+ Internal - External Rotation	Flexion	Adduction	+ Internal - External Rotation
Near 90° Flexion	-.14 (.11)	-.07 (.09)	.81 (.03)	-.46 (.09)	-.21 (.05)	.26 (.01)
One Knee	-.60 (.23)	-.71 (.38)	.92 (.04)	-1.00 (.19)	-.86 (.05)	.32 (.04)
Near Full Flexion	-4.42 (.15)	-1.16 (.04)	.39 (.03)	-4.27 (.23)	-.91 (.06)	-.05 (.03)
Squat	-5.52 (.31)	-1.30 (.08)	-.25 (.03)	-5.85 (.28)	-.79 (.16)	-.32 (.04)
Standing				-1.76 (.08)	.12 (.03)	-.07 (.01)

Table 6: Average net external knee moments normalized by Body weight*Height, Subject 2

Subject 2						
	With Kneepads			Without Kneepads		
	Flexion Moment	+ Abduction - Adduction	Internal Rotation	Flexion	Abduction	Internal Rotation
Near 90° Flexion	-.63 (.10)	-.24 (.01)	.53 (.02)	-3.71 (.06)	.33 (.03)	.54 (.01)
One Knee	-6.45 (.11)	-.69 (.21)	.34 (.04)	-6.05 (.07)	.06 (.1)	.08 (.04)
Near Full Flexion	-3.08 (.05)	.42 (.02)	.25 (.03)	-2.93 (-3.01)	.57 (.58)	.32 (.33)
Squat	-5.51 (.19)	1.21 (.12)	.17 (.03)	-4.49 (.12)	1.90 (.08)	.19 (.03)
Standing				-.17 (.06)	-.28 (.02)	-.04 (.01)

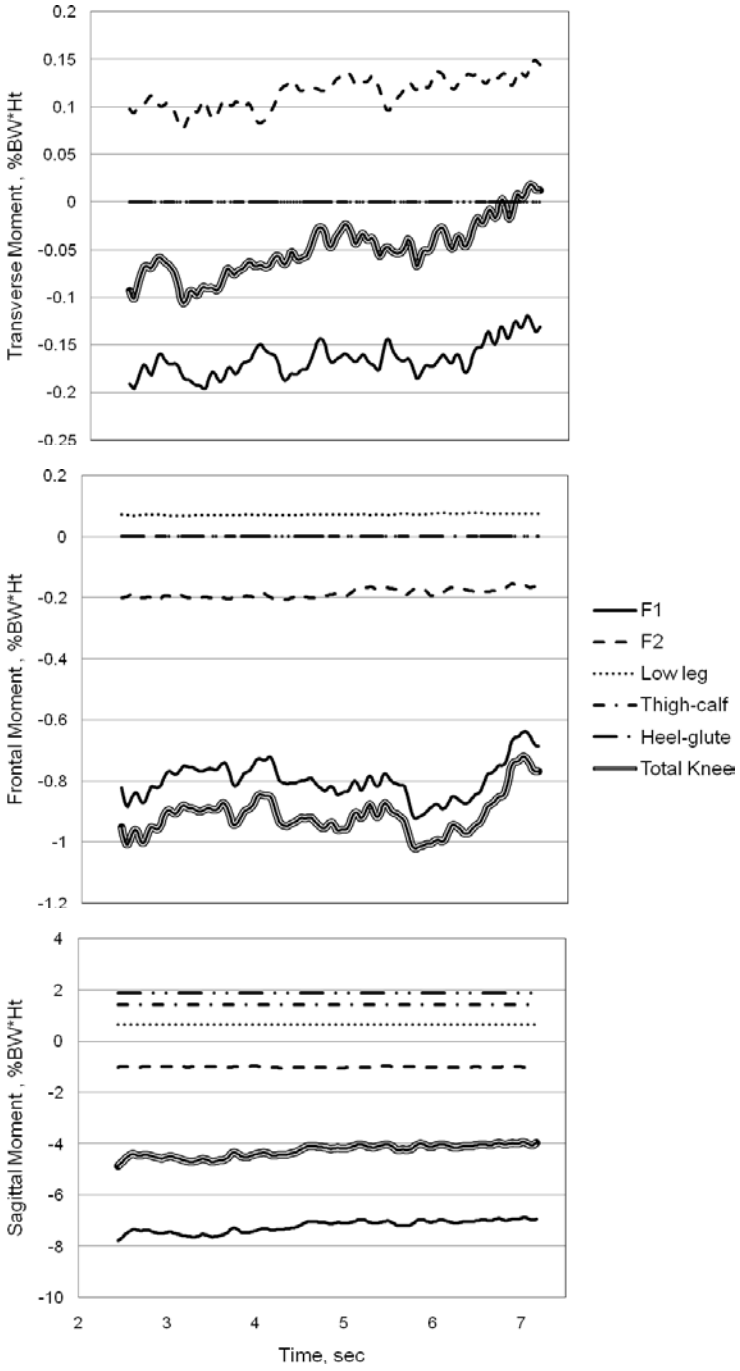

Figure 16: Moment contributions normalized by Bodyweight*Height for Subject 1 kneeling near full flexion without kneepads

4.5 SUMMARY SUBJECT 1

Kneeling near 90° flexion showed the smallest flexion moments, followed by kneeling on one knee, kneeling near full flexion, and squatting. When kneeling near 90° flexion about 47 %BW was placed on the right knee and another 0.27 %BW was placed on the toes. The moments generated by these forces were almost balanced by the weight of the lower leg, creating a net flexion moment of 0.3% BW*Ht. This posture had the smallest abduction moments: 3 Nm without kneepads and 1 Nm with kneepads. External rotation moments were higher with kneepads (10 Nm) than without (3.15 Nm). The higher rotation moment with kneepads was almost entirely due to the moment created by the force at the knee (9.87 Nm). This increase in moment was due to the kneepad changing the COP of the force at the knee. The force in the z-direction moved from 1.4 cm to 3.5 cm medial to the KJC, increasing the abduction moment by nearly 7 Nm.

When kneeling on one knee a predominant amount of weight, 75 %BW, was placed on the knee and a small amount of weight, .54 %BW, was placed on the toes. These forces created a flexion moment which was reduced by the extension moment generated by the weight of the lower leg, creating a mean net flexion moment of 0.8 % BW*Ht. Adduction moments in this posture were lower with kneepads (9 Nm) than without (10 Nm). Internal rotation moments were larger with kneepads (11 Nm) than without (3 Nm). This increase in internal rotation moment was also due to the kneepad changing the location of the COP of the force at the knee from 1.4 cm to 2.9 cm medial to the KJC.

When kneeling near full flexion the weight at the knee was 28 %BW. The weight at the toes was higher than any other kneeling posture, 21 %BW, due to the subject sitting on their heels, applying a force of 8 %BW. The contact between the thigh and the calf was 18 %BW.

The thigh-calf and heel-gluteus contact forces along with the weight of the lower leg created extension moments which acted to stabilize the knee joint in this high flexion posture. The flexion moment generated by the weight at the toes and the knees were still sufficient to create a net flexion moment at the knee of 4 %BW*Ht. Adduction moments were larger with kneepads (14 Nm) than without (11 Nm). When wearing kneepads a 5 Nm internal rotation moment was created and without kneepads a 1 Nm external rotation moment was created. This difference in transverse moments may also be attributed to the COP of the force at the knee moving from 1.3 cm to 4.2 cm medial to the KJC.

Squatting applied a force of 44 %BW to the foot, and created a thigh-calf contact force of 25 %BW. The thigh-calf contact force along with the weight of the lower leg created an extension moment in opposition to the flexion moment created by the ground reaction force at the foot, with a net flexion moment of 6 %BW*Ht. Adduction moments were higher with kneepads (16 Nm) than without (10 Nm). The source of this difference was the x-component of the force at the foot which increased from 20 N without kneepads to 40 N with kneepads. This difference is most likely due to the subjects kneeling posture which may or may not have been directly related to the kneepad. External rotation moments were similar for squatting with (5.5 Nm) and without (5.9 Nm) kneepads.

4.6 SUMMARY SUBJECT 2

Subject 2 showed high variability in knee forces, moments, and angles between kneepad states. When not wearing kneepads the smallest flexion moment was 34 Nm when kneeling near full flexion, followed by 42 Nm when kneeling near 90° flexion, 51 Nm when squatting and the

highest flexion moment was 68 Nm when kneeling on one knee. The largest abduction moments were created when squatting, followed by keeling near full flexion, kneeling near 90° flexion, and kneeling on one knee. Internal rotation moments were largest when kneeling near 90° flexion, followed by kneeling near full flexing, squatting, and kneeling on one knee. When wearing kneepads kneeling near 90° flexion had the smallest flexion moment of 7 Nm, followed by 35 Nm when kneeling near full flexion, 62 Nm when squatting, and 73 Nm when kneeling on one knee. Squatting and kneeling near full flexion created adduction moments and kneeling one knee and kneeling near 90° flexion created adduction moments. Internal rotation moments were largest when kneeling near 90° flexion, followed by kneeling on one knee, kneeling near full flexion, and squatting.

Squatting and kneeling on one knee had the largest flexion moments for both knee pad states. These postures were found to have similar flexion angles: 37° for squatting and 38° for kneeling on one knee. Kneeling on the right knee showed the largest flexion moments because most of their body weight was distributed to their right side. The left leg may have acted to provide balance and stability. Some 60 %BW was distributed to the right side with 40 %BW at the right knee and another 20 %BW at the right toes. This created thigh-calf contact which was not accounted for in the analysis of their data and may have caused an overestimation of the flexion moments. To determine the effect of thigh-calf contact on this moment, the thigh-calf contact moment created in the squatting posture was applied to this posture. When including this contact the flexion moment decreased from 73 Nm to 46 Nm. This new moment is less than squatting (62 Nm), but still higher than that during full flexion (35 Nm).

4.7 STATISTICS

In this study two subjects were asked to simulate 4 postures with and without kneepads while measurements were recorded. To determine the effect of the kneepads on the forces and moments at the knee, multivariate ANOVA was performed for each subject. The mean values of the forces, moments, and angles were compared between kneepad states. A *p*-value of 0.05 was used to demonstrate statistical significance. Table 7 and Table 8 show the resulting p-values from ANOVA where significant values are in bold font.

No significant differences were found between kneepad states for Subject 1. This was expected as Subject 1's posture did not change much (0-4.3° change in joint angles) between kneepad states. Subject 1 showed a significant difference in sagittal moment (p <.001), frontal moment (p = .037), posterior/anterior force (p <.001), distal/proximal force (p <.001), included knee angle (p <.001), and internal/external rotation angle (p = .001) between postures. This was also expected due to the differences in joint angles. Kneeling near 90° flexion created flexion angles of 83°, compared to the 23° of kneeling near full flexion. Internal/external rotation angles also varied between postures and these varied joint angles may have largely contributed to the differences in joint forces and moments between postures.

Subject 2 showed a significant difference in medial/lateral force magnitude between kneepad states (p = .021). This difference is not thought to be a result of the kneepad itself, but of Subject 2 not repeating the postures correctly. When originally instructed to kneel near 90° flexion, their included angle was 85°. When later instructed to kneel their included angle decreased to 39°. This 46° increase in knee flexion, along with the 8° changes in valgus angles may have largely contributed to the significant difference in medial/lateral forces. Subject 1 showed significant differences in frontal moment (p = .040), posterior/anterior force (p = .000),

and distal/proximal force (p = .027) between postures. These differences were also expected as kneeling near 90° flexion and kneeling on one knee created increased posterior forces, and squatting created proximal forces and abduction moments compared to the distal forces and adduction moments created in some other postures.

Table 7: Resulting p-values for ANOVA, Subject 1

Subject 1			
		Kneepad	Posture
Moments	Sagittal	.908	**<.001**
	Frontal	.727	**.037**
	Transverse	.221	.148
Forces	Medial/Lateral	.443	.288
	Posterior/Anterior	.934	**<.001**
	Distal/Proximal	.982	**<.001**
Angles	Included	.948	**<.001**
	Varus/Valgus	.801	.485
	Int/Ext Rotation	.984	**.001**

Table 8: Resulting p-values for ANOVA, Subject 2

Subject 2			
		Kneepad	Posture
Moments	Sagittal	.795	.074
	Frontal	.387	**.040**
	Transverse	.776	.065
Forces	Medial/Lateral	**.021**	.692
	Posterior/Anterior	.967	**<.001**
	Distal/Proximal	.546	**.027**
Angles	Included	.339	.392
	Varus/Valgus	.276	.564
	Int/Ext Rotation	.125	.521

Data from Subject 1 and Subject 2 were combined to see if there was a significant difference in forces, moments, and joint angles due to the interaction of kneepad and posture. No significant differences were found, Table 9.

Table 9: Resulting p-values for ANOVA of Kneepad*Posture Interaction, Subjects 1&2

		Kneepad*Posture Interaction
Moments	Sagittal	.903
	Frontal	.993
	Transverse	.758
Forces	Medial/Lateral	.970
	Posterior/Anterior	.964
	Distal/Proximal	.805
Angles	Included	.802
	Varus/Valgus	.153
	Int/Ext Rotation	.929

ANOVA was also performed to determine if significant differences existed between Subject 1 and Subject 2. Significant differences in all moments, posterior forces, and included angles were shown to exist, Table 10.

Table 10: Resulting p-values for ANOVA, Subject comparison

		p-value
Moments	Sagittal	**<.001**
	Frontal	**<.001**
	Transverse	**<.001**
Forces	Medial/Lateral	.65
	Posterior/Anterior	**<.001**
	Distal/Proximal	.16
Angles	Included	**<.001**
	Varus/Valgus	.06
	Int/Ext Rotation	.52

5.0 SENSITIVITY ANALYSIS

To determine the major sources of error in the moment calculations, sensitivity analyses were performed. An analysis of the model parameters was performed for each posture to determine the effect of varying the moment arms and forces on the sagittal moments. Another analysis was performed, varying the location of the knee joint center and measuring its effect on the knee moments. All mean values used in this analysis were from Subject 1 without kneepads.

5.1 VARYING MODEL PARAMETERS

The mean values of the z-components of the moment arms and the y-components of the forces were varied to determine their effect on the sagittal knee moments. Although static postures were studied there was some expected motion of the markers due to motion artifact and the subject maintaining balance. The motion of the markers was shown to be less than 1.5 cm over the course of a squatting trial. To include this source of error the moment arms were varied by ± 1-3 cm in 1 cm increments. One force plate in the laboratory had a threshold of approximately 3 N. To account for this error, the forces were varied by ± 2-6 N in 2 N increments. External force diagrams for all postures are shown in Figure 16. Plots of the varied parameters and resulting moments for kneeling near 90° flexion, kneeling on one knee, kneeling near full flexion, and squatting are shown in Figure 17, Figure 18, Figures 19 and 20, and Figure 21,

respectively. In all figures the blue diamond represents the mean value of the model parameter and its corresponding sagittal moment. The pink squares represent the sagittal moments resulting from varying the parameter. The green line connecting the green triangles represents the standard deviation of the model parameter. This illustrates the amount of variability of the sagittal moment that is expected due to the model parameter. Table 10 shows the sensitivity of the sagittal moments to the model parameters. Varied moment arms resulted in sensitivities with units of Nm/cm. Varied moment arm results in change in moment per centimeter and varied forces results in change in moment per Newton. Also shown are the percentages of change in sagittal moment per centimeter or per Newton. Parameters creating the largest changes in moments are shown in bold. Parameters with the least change in moment are shown in italics.

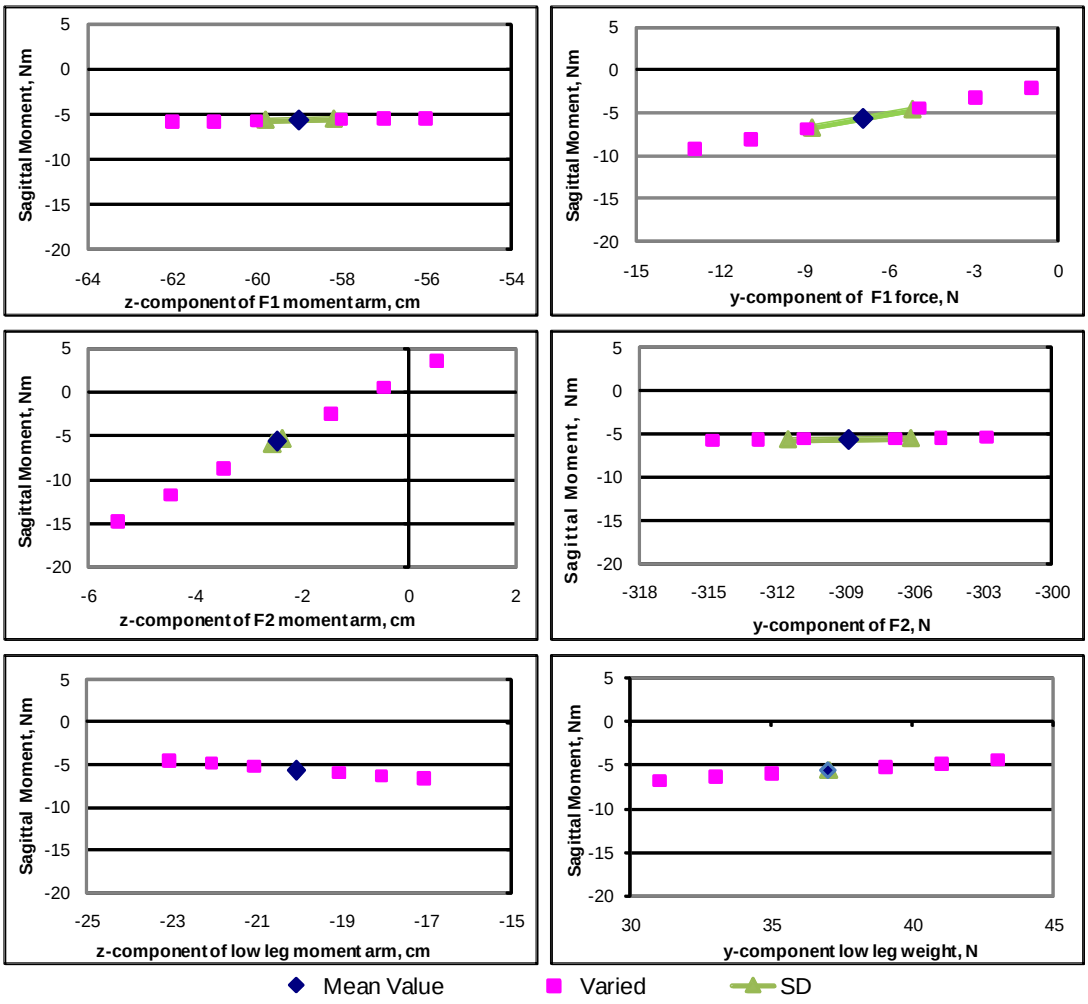

Figure 17: Varied forces and moment arms and corresponding sagittal knee moments for kneeling near 90° flexion. The forces and moment arms were varied for the ground reaction force at the toes (F1), the ground reaction force at the right knee (F2), and the weight of the foot+shank (low leg). Note that all moment arm values are shown in cm, all forces are shown in N, and all moments are not normalized and are shown in Nm. Varying the z-component of the F1 moment arm by 3 cm changed the sagittal knee moment by .2 Nm. When F1 was varied by 6 N, the moment changed by 3.5 Nm. Varying the z-component of the F2 moment arm by 3 cm was sufficient to more than triple the magnitude of the sagittal moment and change its interpretation. Varying the y-component of the F2 force by 6 N, changed the sagittal moment by .1 Nm. Varying the z-component of the COM of the lower leg by 3 cm changed the moment by 1.1 Nm. Varying the y-component of the low leg weight changed the moment by 1.2 Nm.

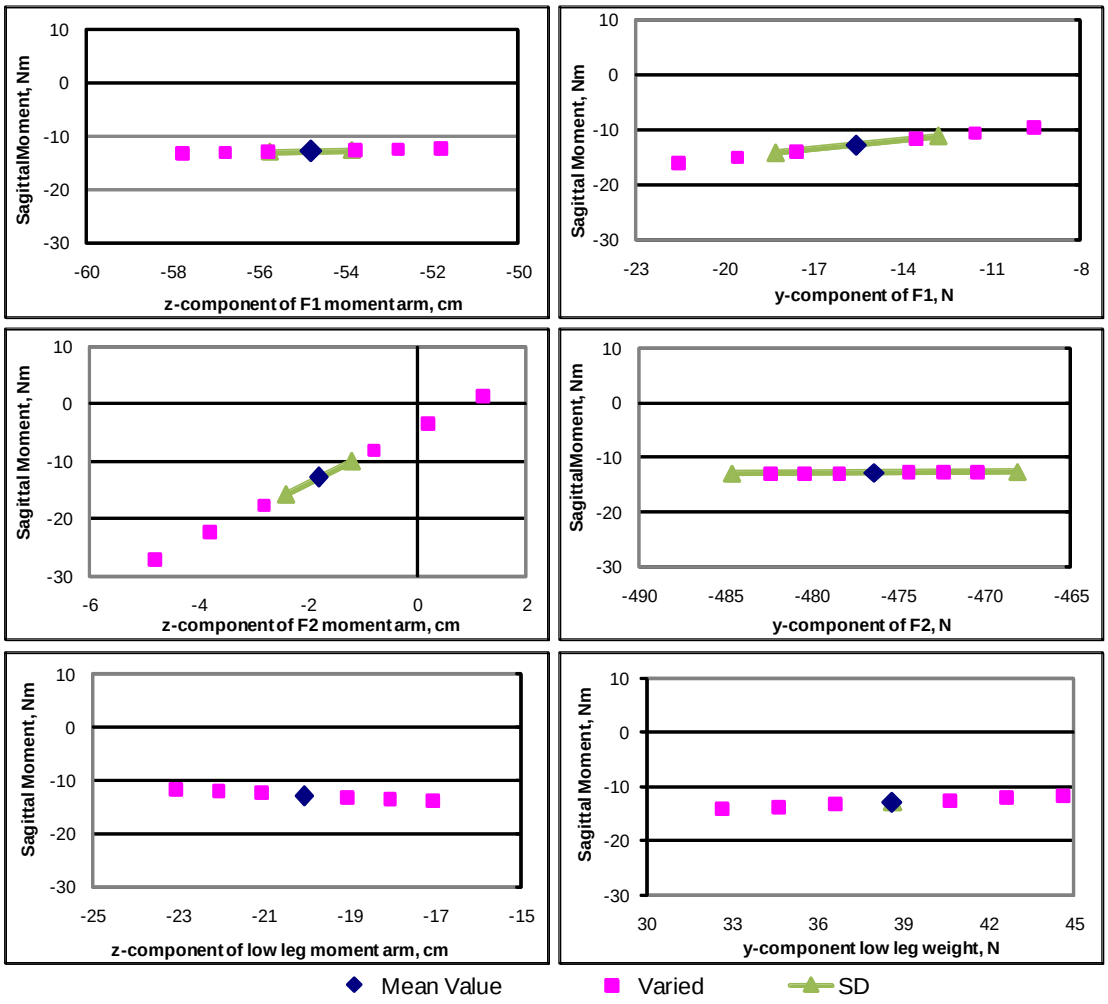

Figure 18: Varied forces and moment arms and corresponding sagittal knee moments for kneeling on the right knee. The forces and moment arms were varied for the ground reaction force at the toes (F1), the ground reaction force at the right knee (F2), and the weight of the foot+shank (low leg). Varying the z-component of the F1 moment arm by 3 cm, changed the sagittal moment by .5 Nm. Varying the y-component of F1 by 6 N, changed the sagittal moment by 3.3 Nm. Decreasing the z-component of the F2 moment arm by 3 cm more than doubled the sagittal moment. When this moment arm was increased by 3 cm, an extension moment was created. Varying the y-component of F2 by 6 N changed the moment by .1 Nm. Varying the z-component of the low leg COM by 3 cm and the y-component of the low leg weight by 6 N changed the moment by 1.2 Nm.

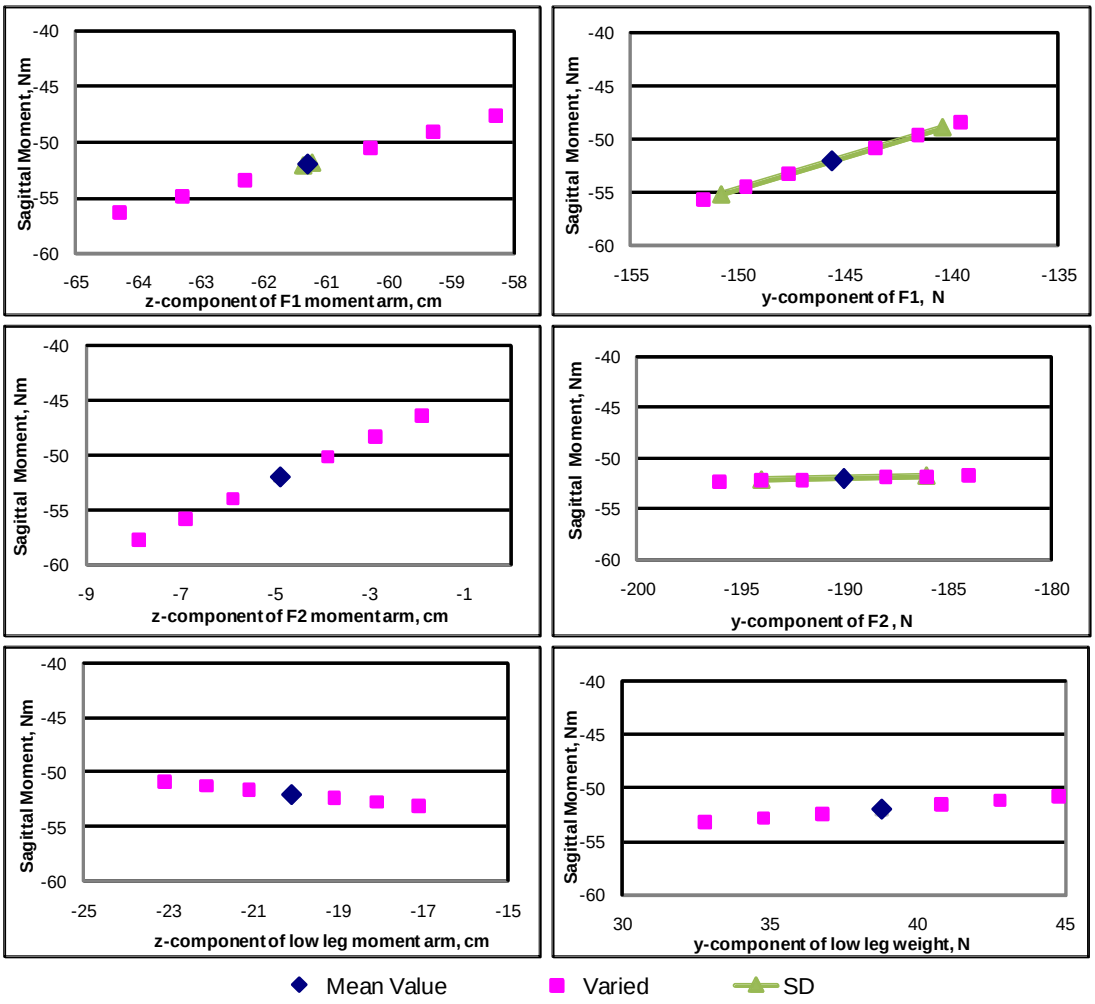

Figure 19: Varied forces and moment arms and corresponding sagittal knee moments for kneeling near full flexion. The forces and moment arms were varied for the ground reaction force at the toes (F1), the ground reaction force at the right knee (F2), and the weight of the foot+shank (low leg), the thigh-calf contact force, and the heel-gluteus contact force. Varying the z-component of the F1 moment arm by 3 cm changed the moment by 4.4 Nm. Varying the y-component of F1 by 6 N changed the moment by 3.7 Nm. Varying the z-component of the F2 moment arm by 3 cm changed the moment by 5.7 Nm. Varying the y-component of F2 by 6 N changed the moment by .3 N. Varying the z-component of the low leg COM by 3 cm changed the moment by 1.2 Nm. Varying the y-component of the low leg weight by 6 N changed the moment by 1.2 Nm.

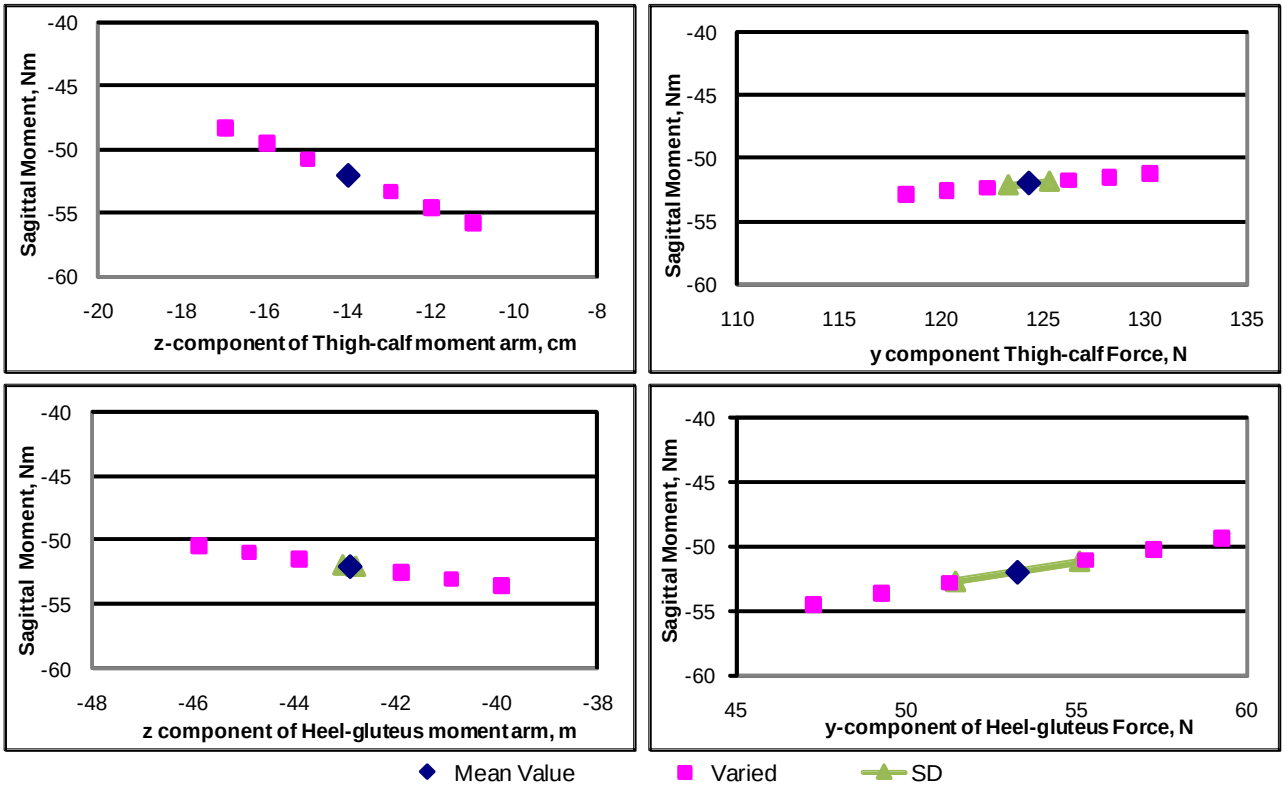

Figure 20: Varied forces and moment arms and corresponding sagittal knee moments for kneeling near full flexion, continued. The forces and moment arms were varied for the ground reaction force at the toes (F1), the ground reaction force at the right knee (F2), and the weight of the foot+shank (low leg), the thigh-calf contact force, and the heel-gluteus contact force. Varying the z-component of the thigh-calf moment arm by 3 cm changed the moment by 3.7 Nm. Varying the thigh-calf contact force by 6 N changed the moment by .8 Nm. Varying the heel-gluteus moment arm by 3 cm changed the moment by 1.5 Nm. Varying the heel-gluteus contact force by 6 N changed the moment by 2.5 Nm.

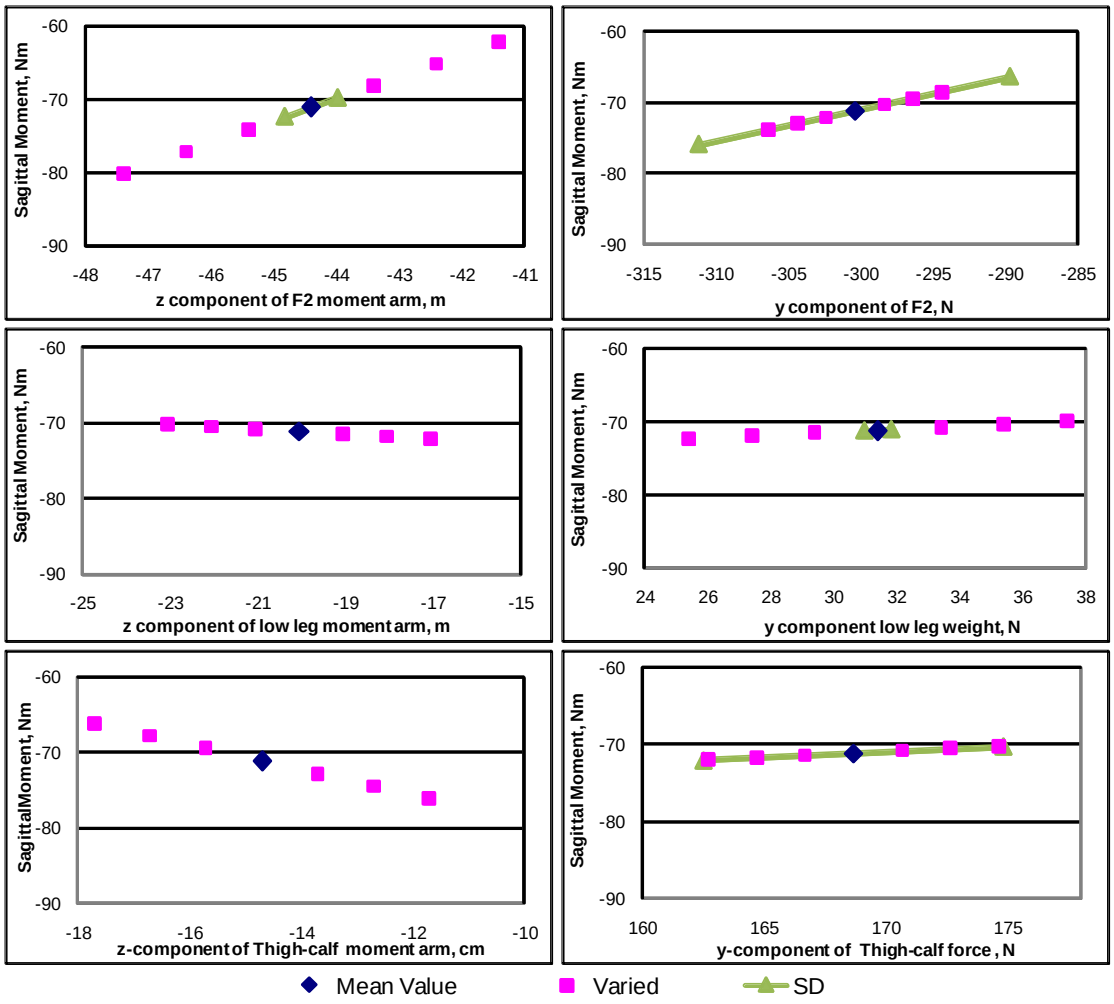

Figure 21: Varied forces and moment arms and corresponding sagittal knee moments for squatting. The forces and moment arms were varied for the ground reaction force at the foot (F1), the weight of the foot+shank (low leg), and the thigh-calf contact force. Varying the z-component of the F2 moment arm by 3 cm, changed the moment by 9 Nm. Varying the y-component of F2 by 6 N, changed the moment by 2.7 Nm. Varying the z-component of the low leg COM by 3 cm, changed the moment by .9 Nm. Varying the y-component of the low leg weight by 6 N, changed the moment by 1.2 Nm. Varying the z-component of the thigh-calf moment arm by 3 cm, changed the moment by 5.1 Nm. Varying the y-component of the thigh-calf contact force by 6 N, changed the moment by .9 Nm.

Table 11: Sensitivity of sagittal moments to changes in model parameters for all postures

	Varied Parameter	Model Sensitivity
Near 90° Flexion	F1 moment arm	.06 Nm/cm 1.13 %/cm
	F1	.55 Nm/N 10.5 %/N
	F2 moment arm	**3.1 Nm/cm** **55 %/cm**
	F2	*.03 Nm/N* *.44 %/N*
	low leg moment arm	-.35 Nm/cm -6.2 %/cm
	low leg weight	-.2 Nm/N -3.6 %/N
One Knee	F1 moment arm	.16 Nm/cm 1.2 %/cm
	F1	.55 Nm/N 4.8 %/N
	F2 moment arm	**4.8 Nm/cm** **37 %/cm**
	F2	*.02 Nm/N* *.13 %/N*
	low leg moment arm	-.39 Nm/cm -3 %/cm
	low leg weight	-.2 Nm/N -1.6 %/N
Squat	**F2 moment arm**	**3 Nm/cm** **4.2 %/cm**
	F2	.4 Nm/N .55 %/N
	low leg moment arm	-.31 Nm/cm -.44 %/cm
	low leg weight	-.2 Nm/N -.27 %/N
	Thigh-calf moment arm	-1.7 Nm/cm -2.4 %/cm
	Thigh-calf Force	*-.15 Nm/N* *-.2 %/N*

Table 11 (continued).

Near Full Flexion	F1 moment arm	1.5 Nm/cm 2.8 %/cm
	F1	.61 Nm/N 1.7 %/N
	F2 moment arm	**1.9 Nm/cm** **3.7 %/cm**
	F2	*.05 Nm/N* *.1 %/N*
	low leg moment arm	-.39 Nm/cm -.75 %/cm
	low leg weight	-.2 Nm/N -.38 %/N
	Thigh-calf moment arm	-1.2 Nm/cm -2.4 %/cm
	Thigh-calf force	-.14 Nm/N -.27 %/N
	Heel-gluteus moment arm	-.44 Nm/cm -.84 %/cm
	Heel-gluteus force	-.48 Nm/N -.9 %/N

In the kneeling near 90° flexion model, the location of the force at the knee (F2) increasing the sagittal knee moment by 3.1 Nm per every centimeter this force was moved distally. The sagittal moment was the least sensitive to the force at the knee; increasing by.03 Nm for every 1 N increase in force. Similarly to the kneeling near 90 flexion model, the kneeling on one knee model was the most sensitive to the location of the force at the knee; increasing by 4.8 Nm with every 1 cm this force was moved distally. The sagittal moment was the least sensitive to the force at the knee, increasing by .02 Nm with a 1 N increase in force. In the squatting model, the sagittal moment was the most sensitive to the location of the force at the foot, increasing by 3 Nm for every 1 cm this force was moved distally. The sagittal moment was the least sensitive to the thigh-calf contact force; decreasing by .15 Nm with every 1 N this force

was increased. In the kneeling near full flexion model, the sagittal moment was the most sensitive to the location of the force at the knee increasing by 1.9 Nm for every 1 cm this force was moved distally. The sagittal moment was least sensitive to the force at the knee; increasing by .05 Nm for every 1 N increase in force. Moving the location of the thigh-calf contact force 1 cm distally decreased sagittal moments by more than 1 Nm in the kneeling near full flexion and squatting models.

5.2 VARYING KNEE JOINT CENTER LOCATION

Knee joint center (KJC) locations are dependent on the placement of surface markers by laboratory researchers. Although one researcher was responsible for palpating the medial and lateral epicondyles of the femur, some variation in the placement of these markers was expected. This variation in marker placement will affect the location of the KJC, thereby affecting all moment calculations. A sensitivity analysis was performed on the KJC location to determine the effect of its variation on the knee moments. The KJC was varied by ±3 cm along the anatomical shank axes. Changes in the KJC locations resulted in linear changes in the joint moments. Plots showing varied KJC locations and resulting moments for kneeling near 90° flexion, kneeling on one knee, kneeling near full flexion and squatting are shown in Figure 22, Figure 23, Figure 24, and Figure 25, respectively. Percent change in moments resulting from variation in KJC locations for these postures are shown in Table 8, Table 9, Table 10, and Table 11, respectively. Although no moments changed by an order of magnitude, some variations were sufficient to change the interpretation of the moments.

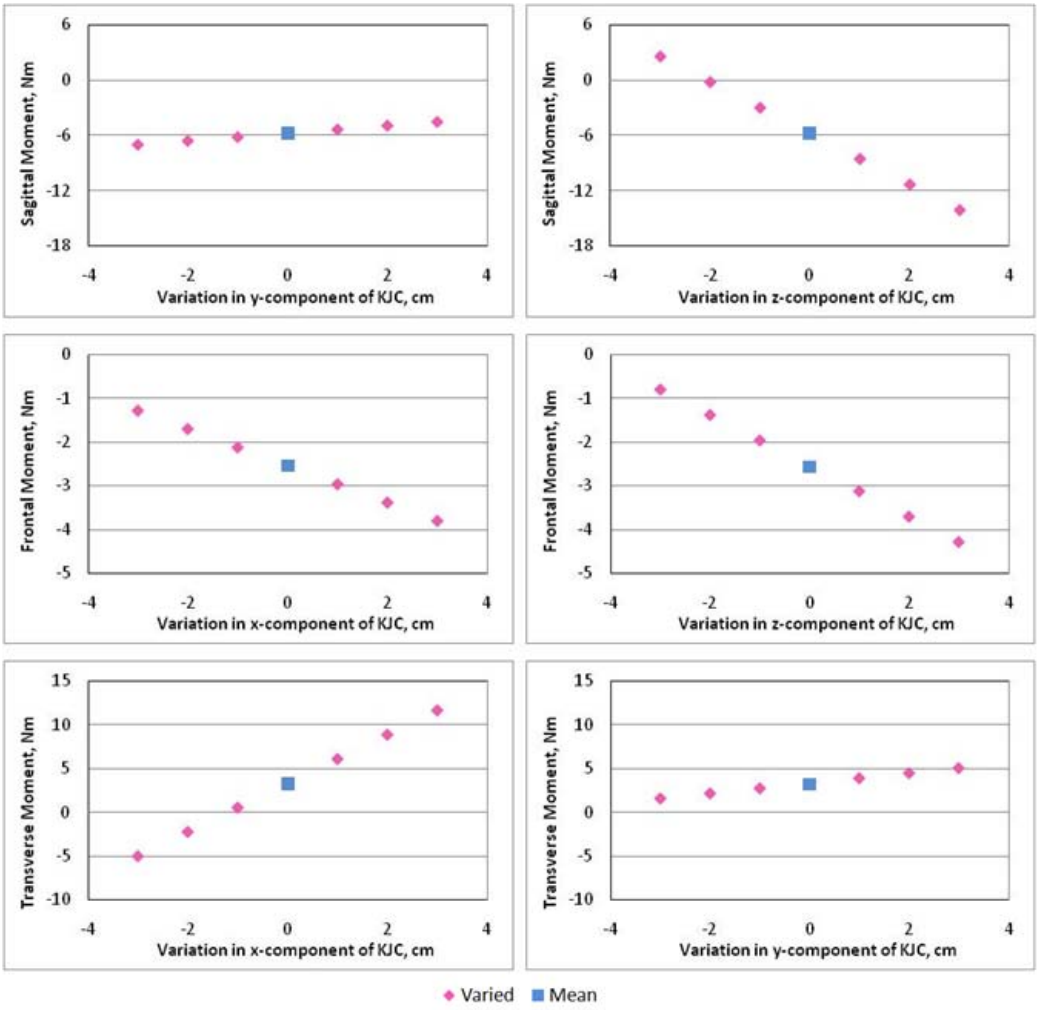

Figure 22: Varied KJC locations and resulting knee moments for kneeling near 90° flexion. Varying the x, y, and z-components of the KJC location had no effect on the sagittal, frontal, and transverse moments, respectively. Varying the y-component by 3 cm changed the sagittal moment by 1.3 Nm. Varying the z-component by 3 cm more than doubled the sagittal moment. Varying the x-component by 3 cm changed the frontal moment by 1.3 Nm. Varying the z-component by 3 cm changed the adduction moment by 1.7 Nm. Varying the x-component by 3 cm and varying the y-component by 3cm more than doubled the transverse moment and changed the interpretation of this moment.

Sagittal moments were most sensitive to the z-location of the KJC when kneeling near 90° flexion. This moment increased from a 5.7 Nm to a 14 Nm flexion moment when the KJC was moved 3 cm anterior. When the KJC was moved 3 cm posterior the moment decreased to a 2.6 Nm extension. Adduction moments were most sensitive to the z-location of the KJC, increasing from 2.5 Nm to 4.3 Nm when the KJC was moved 3 cm posterior, and decreasing to .8 Nm when the KJC was moved 3 cm anterior. Transverse moments were most sensitive to the x-position of the KJC increasing from 3.3 Nm to 11.6 Nm when the KJC was moved 3 cm lateral. This moment became an external rotation moment of 5.1 Nm when the KJC was moved 3 cm medial.

Table 12: Percent change in moments due to varying KJC for kneeling near 90 degrees flexion

Varied by, m	Change in Moment, %		
	Sagittal	Frontal	Transverse
[.01, 0, 0]	0.00	-16.46 %/cm	84.87 %/cm
[.02, 0, 0]	0.00	-32.91	169.73
[.03, 0, 0]	0.00	-49.37	254.60
[-.01, 0, 0]	0.00	16.46	-84.87
[-.02, 0, 0]	0.00	32.91	-169.74
[-.03, 0, 0]	0.00	49.37	-254.60
[0, .01, 0]	7.29	0.00	17.70
[0, .02, 0]	14.59	0.00	35.39
[0, .03, 0]	21.88	0.00	53.09
[0, -.01, 0]	-7.29	0.00	-17.70
[0, -.02, 0]	-14.59	0.00	-35.39
[0, -.03, 0]	-21.88	0.00	-53.09
[0, 0, .01]	-48.52	-22.83	0.00
[0, 0, .02]	-97.04	-45.66	0.00
[0, 0, .03]	-145.56	-68.48	0.00
[0, 0, -.01]	48.52	22.83	0.00
[0, 0, -.02]	97.04	45.65	0.00
[0, 0, -.03]	145.57	68.48	0.00

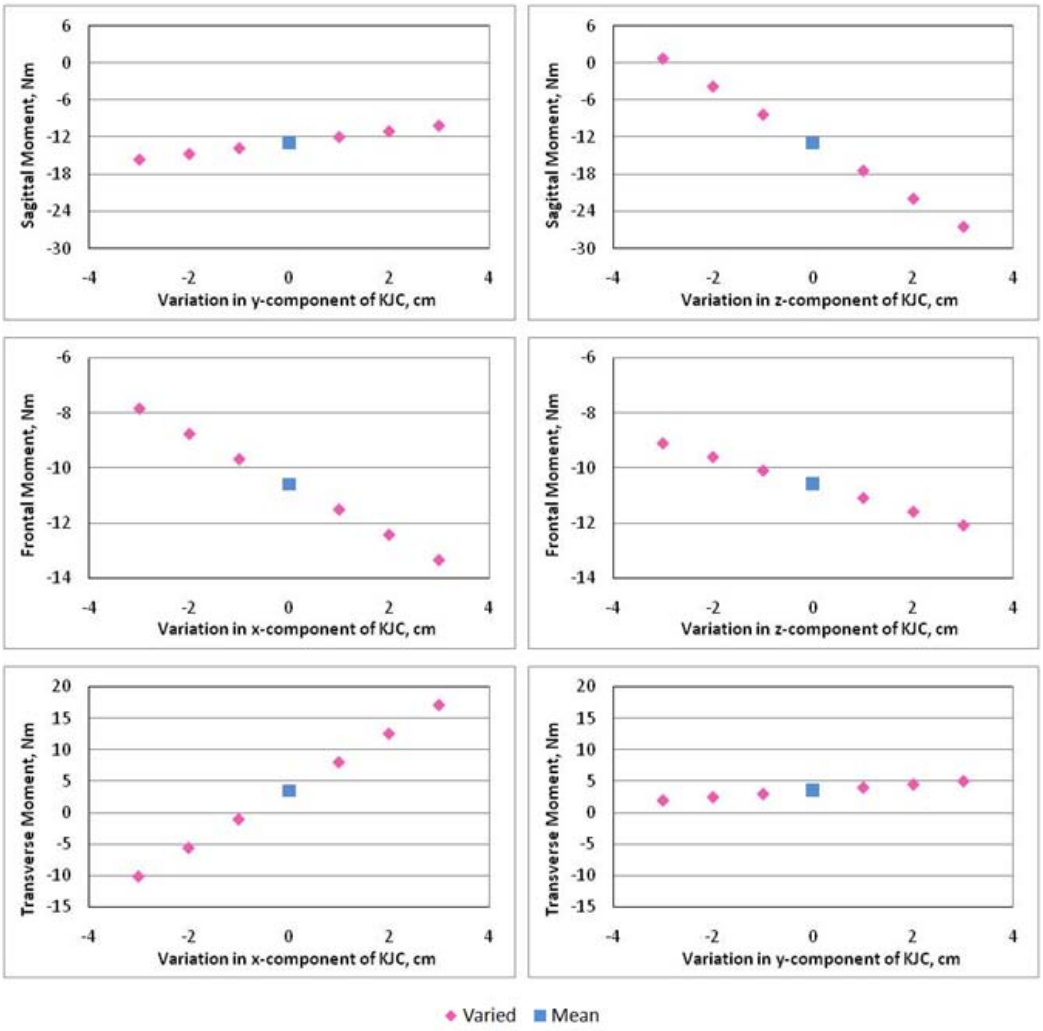

Figure 23: Varied KJC locations and resulting knee moments for kneeling on right knee. Varying the x, y, and z-components of the KJC location had no effect on the sagittal, frontal, and transverse moments, respectively. Varying the y-component by 3 cm changed the flexion moment by 2.7 Nm. Varying the z-component by 3 cm changed the sagittal moment by 13.6 Nm and changed it interpretation. Varying the x-component by 3 cm changed the adduction moment by 2.7 Nm. Varying the z-component changed the frontal moment by 1.5 Nm. Varying the x-component by 3 cm changed the transverse moment by 9.1 Nm. Varying the y-component by 3 cm changed the transverse moment by 1.5 Nm.

Flexion moments were most sensitive to the z-location of the KJC when kneeling on one knee. This moment increased from 12.8 Nm to 26 Nm when the KJC was moved 3 cm anterior. When the KJC was moved 3 cm posterior the moment became a .78 Nm extension moment. Adduction moments were most sensitive to the x-location of the KJC. Increasing from 10.6 Nm to 13.3 Nm when the KJC was moved 3 cm anterior, and decreasing to 7.8 Nm when the KJC was moved 3 cm posterior. Transverse moments were most sensitive to the x-position of the KJC. The internal rotation moment changed from 3.5 Nm to 17.1 Nm when the KJC was moved 3 cm medial. This moment became an external rotation moment of 10.1 Nm when the KJC was moved 3 cm lateral.

Table 13: Percent change in moments due to varying KJC for kneeling on one knee

Varied by, m	Change in Moment, %		
	Sagittal	Frontal	Transverse
[.01, 0, 0]	0.00	-8.64	129.27
[.02, 0, 0]	0.00	-17.28	258.54
[.03, 0, 0]	0.00	-25.91	387.81
[-.01, 0, 0]	0.00	8.64	-129.27
[-.02, 0, 0]	0.00	17.28	-258.54
[-.03, 0, 0]	0.00	25.91	-387.81
[0, .01, 0]	7.13	0.00	14.28
[0, .02, 0]	14.27	0.00	28.56
[0, .03, 0]	21.40	0.00	42.84
[0, -.01, 0]	-7.13	0.00	-14.28
[0, -.02, 0]	-14.27	0.00	-28.56
[0, -.03, 0]	-21.40	0.00	-42.84
[0, 0, .01]	-35.36	-4.73	0.00
[0, 0, .02]	-70.71	-9.46	0.00
[0, 0, .03]	-106.07	-14.19	0.00
[0, 0, -.01]	35.36	4.73	0.00
[0, 0, -.02]	70.71	9.46	0.00
[0, 0, -.03]	106.07	14.19	0.00

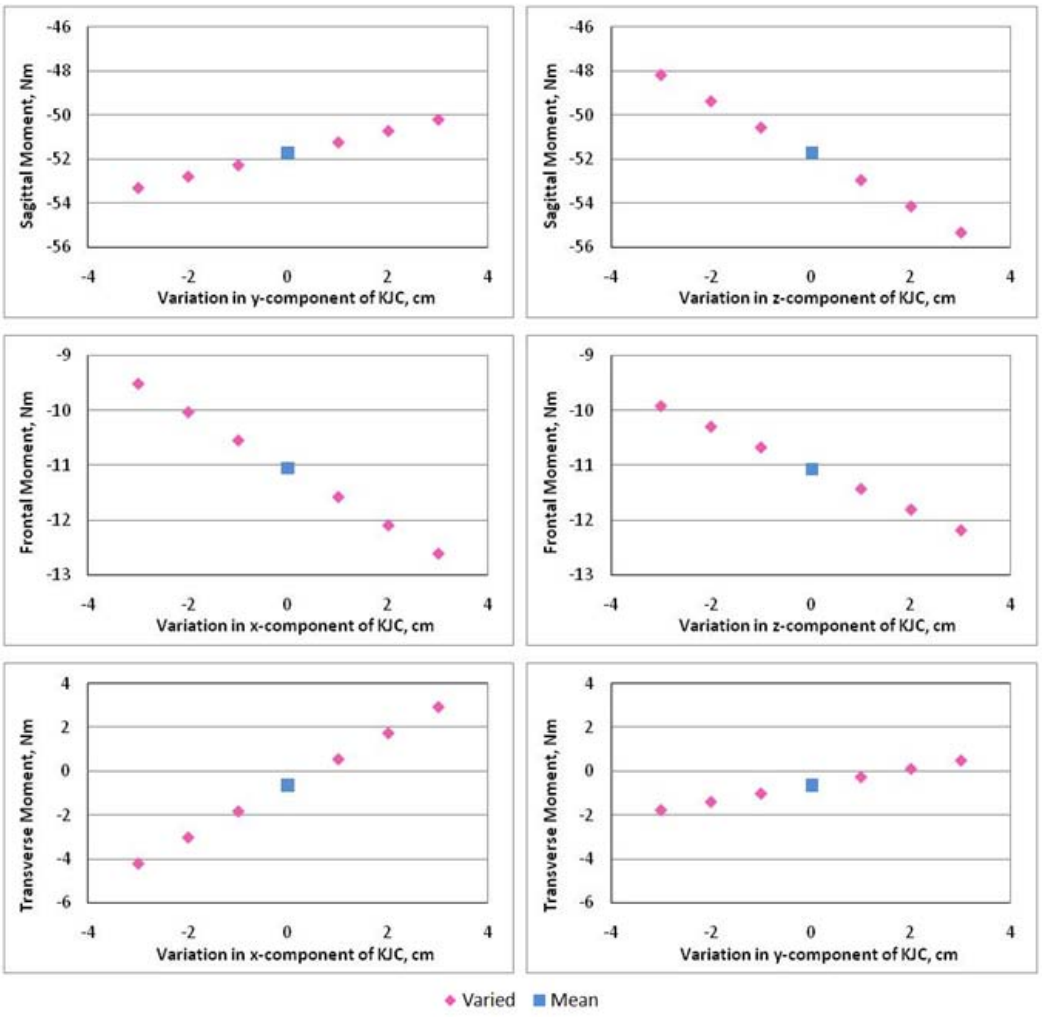

Figure 24: Varied KJC locations and resulting knee moments for kneeling near full flexion. Varying the x, y, and z-components of the KJC location had no effect on the sagittal, frontal, and transverse moments, respectively. Varying the y-component by 3 cm changed the flexion moment by 1.6 Nm. Varying the z-component by 3 cm changed the flexion moment by 3.6 Nm. Varying the x-component by 3 cm changed the adduction moment by 1.6 Nm. Varying the z-component by 3 cm changed the adduction moment by 1.1 Nm. Varying the x-component by 3 cm changed the transverse moment by 3.6 Nm and changed its interpretation. Varying the y-component by 3 cm changed the transverse moment by 1.4 Nm and changed its interpretation.

Flexion moments were most sensitive to the z-location of the KJC when kneeling near full flexion. This moment increased from 51.75 Nm to 55 Nm when the KJC was moved 3 cm anterior and decreased to 48.2 Nm when the KJC was moved 3 cm posterior. Adduction moments were most sensitive to the x-location of the KJC, increasing from 11.1 Nm to 12.6 Nm when the KJC was moved 3 cm lateral, and decreasing to 9.5Nm when the KJC was moved 3 cm medial. Transverse moments were most sensitive to the x-position of the KJC. The external rotation moment increased from .65 Nm to 4.2 Nm when the KJC was moved 3 cm medial. This moment became an internal rotation moment of 2.93 Nm when the KJC was moved 3 cm lateral.

Table 14: Percent change in moments due to varying KJC for kneeling near full flexion

Varied by, m	Change in Moment, %		
	Sagittal	Frontal	Transverse
[.01, 0, 0]	0.00	-4.66	184.53
[.02, 0, 0]	0.00	-9.35	369.06
[.03, 0, 0]	0.00	-14.02	553.59
[-.01, 0, 0]	0.00	4.67	-184.55
[-.02, 0, 0]	0.00	9.35	-369.07
[-.03, 0, 0]	0.00	14.02	-553.60
[0, .01, 0]	0.99	0.00	58.59
[0, .02, 0]	1.99	0.00	117.17
[0, .03, 0]	2.99	0.00	175.76
[0, -.01, 0]	-1.00	0.00	-58.60
[0, -.02, 0]	-2.00	0.00	-117.19
[0, -.03, 0]	-3.00	0.00	-175.77
[0, 0, .01]	-2.31	-3.43	0.00
[0, 0, .02]	-4.61	-6.85	0.00
[0, 0, .03]	-6.92	-10.28	0.00
[0, 0, -.01]	2.30	3.43	0.00
[0, 0, -.02]	4.61	6.85	0.00
[0, 0, -.03]	6.91	10.28	0.00

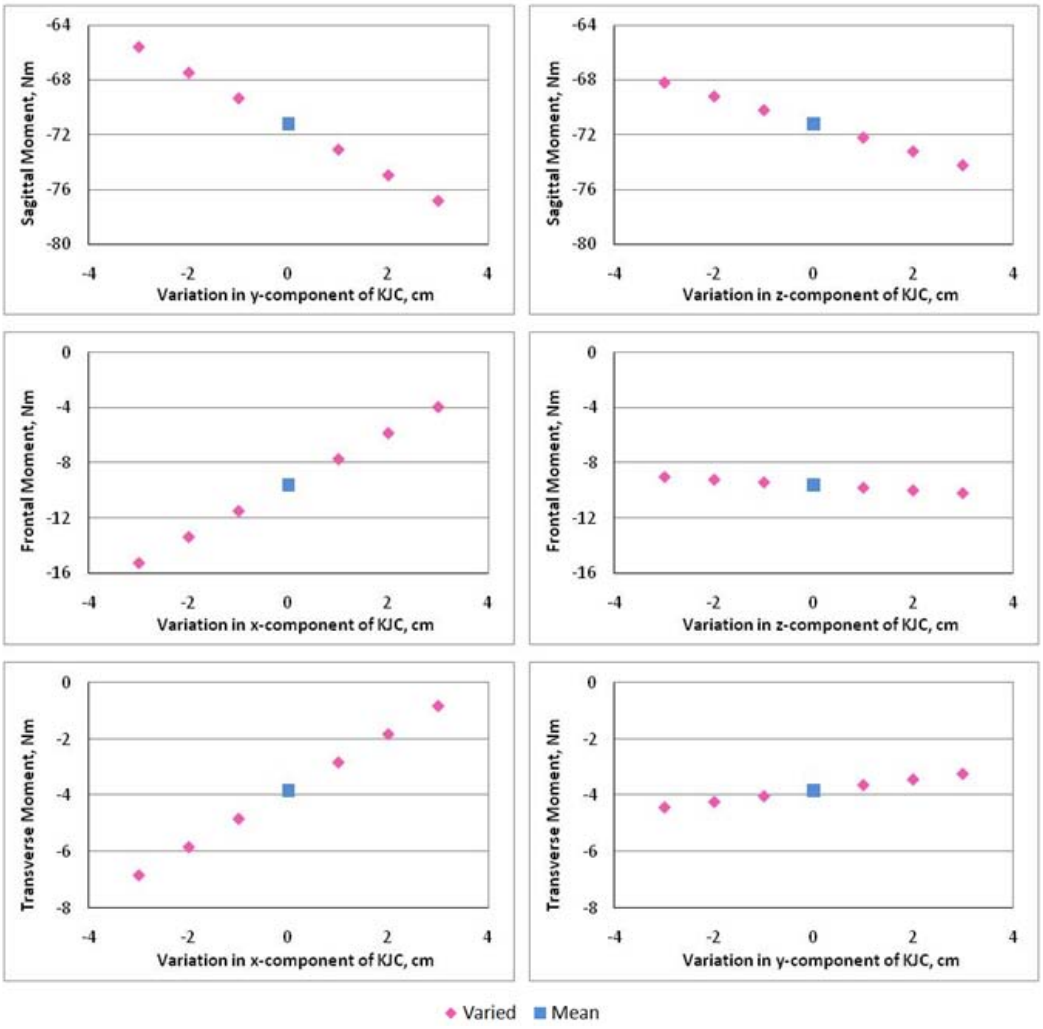

Figure 25: Varied KJC locations and resulting knee moments for squatting. Varying the x, y, and z-components of the KJC location had no effect on the sagittal, frontal, and transverse moments, respectively. Varying the y-component by 3 cm changed the flexion moment 5.6 Nm. Varying the z-component by 3 cm changed the flexion moment by 3 Nm. Varying the x-component by 3 cm changed the adduction moment by 5.6 Nm. Varying the z-component by 3 cm changed the adduction moment by 0.6 Nm. Varying the x-component by 3 cm changed the transverse moment by 3 Nm. Varying the y-component by 3 cm changed the external rotational moment by .6 Nm.

Flexion moments were most sensitive to the y-location of the KJC when squatting. This moment increased from 71.2 Nm to 76.9 Nm when the KJC was moved 3 cm superior. When the KJC was moved 3 cm inferior the moment decreased to 65.6 Nm. Adduction moments were most sensitive to the x-location of the KJC. Increasing from 9.59 Nm to 15.2 Nm when the KJC was moved 3 cm medial, and decreasing to 3.9 Nm when the KJC was moved 3 cm lateral. Transverse moments were most sensitive to the x-position of the KJC. The external rotation moment increased from 3.8 Nm to 6.8 Nm when the KJC was moved 3 cm medial and decreased to .8 Nm when the KJC was moved 3 cm lateral.

Table 15: Percent change in moments due to varying KJC for squatting

Varied by, m	Change in Moment, %		
	Sagittal	Frontal	Transverse
[.01, 0, 0]	0.00	19.61	26.12
[.02, 0, 0]	0.00	39.22	52.23
[.03, 0, 0]	0.00	58.82	78.35
[-.01, 0, 0]	0.00	-19.61	-26.12
[-.02, 0, 0]	0.00	-39.21	-52.23
[-.03, 0, 0]	0.00	-58.82	-78.35
[0, .01, 0]	-2.64	0.00	5.16
[0, .02, 0]	-5.28	0.00	10.32
[0, .03, 0]	-7.92	0.00	15.48
[0, -.01, 0]	2.64	0.00	-5.16
[0, -.02, 0]	5.28	0.00	-10.32
[0, -.03, 0]	7.92	0.00	-15.48
[0, 0, .01]	-1.41	-2.06	0.00
[0, 0, .02]	-2.82	-4.13	0.00
[0, 0, .03]	-4.22	-6.20	0.00
[0, 0, -.01]	1.41	2.07	0.00
[0, 0, -.02]	2.82	4.13	0.00
[0, 0, -.03]	4.22	6.20	0.00

Summaries of model sensitivities to KJC locations for all postures are shown in Table 16. Values are shown due to varying KJC locations by 1 cm in the lateral, anterior, and proximal directions. Sensitivity values are shown in Nm changes per cm and percentage of moment change per cm. Greatest changes in moments are shown in bold. The largest sensitivities where shown in the transverse moments due to moving the KJC 1 cm laterally in all postures.

Table 16: Sensitivity of moments to KJC location for all postures

Posture	Varied direction	Sensitivity (Nm/cm & %/cm) of Moments		
		Sagittal	Frontal	Transverse
Kneeling Near 90° Flexion	lateral	no change	.42 Nm/cm -16.5 %/cm	**2.8 Nm/cm** **84.9 %/cm**
	anterior	.42 Nm/cm 7.3 %/cm	no change	.58 Nm/cm 17.7 %/cm
	proximal	-2.8 Nm/cm -48.5 %/cm	-.58 Nm/cm -22.8 %/cm	no change
Kneeling on One Knee	lateral	no change	-.9 Nm/cm -8.6 %/cm	**4.5 Nm/cm** **129.3 %/cm**
	anterior	.92 Nm/cm 7.1 %/cm	no change	.5 Nm/cm 14.3 %/cm
	proximal	-4.5 Nm/cm -35.4 %/cm	-.5 Nm/cm -4.7 %/cm	no change
Squatting	lateral	no change	1.89 Nm/cm 19.6 %/cm	**1 Nm/cm** **26.1 %/cm**
	anterior	-1.9 Nm/cm -2.6 %/cm	no change	.20 Nm/cm 5.2 %/cm
	proximal	-1 Nm/cm -1.4 %/cm	-.2 Nm/cm -2.1 %/cm	no change
Kneeling Near Full Flexion	lateral	no change	-.52 Nm/cm -4.7 %/cm	**1.2 Nm/cm** **184.5 %/cm**
	anterior	1 Nm/cm 1 %/cm	no change	.38 Nm/cm 58.6 %/cm
	proximal	-1.2 Nm/cm -2.3 %/cm	-.38 Nm/cm -3.4 %/cm	no change

6.0 MODEL VALIDATION

The developed computational model is based on techniques which have been previously used to determine the 3D joint moments in gait analysis. However, due to the complexity of using segment coordinate systems, the model was validated by several means. To ensure accuracy of the anatomical coordinate system calculations, the origin of the anatomical coordinate system was verified to equal to the KJC. The KJC location in the GCS was multiplied by $[T_{GAshank}]^{-1}$. The result was point [0 0 0], thereby validating the KJC as the origin of the ASCS.

Due to the lack of research on kneeling knee forces and moments, no direct comparisons could be made to force and moment values reported in literature. Instead the force and moment calculations were validated by determining the forces and moments during quiet standing and comparing these values to published research. Quiet standing produced a mean flexion moment of .27 Nm/kg, a mean adduction moment of .15 Nm/kg, and a mean internal rotational moment of .04 Nm/kg applied to the knee joint. These values were also comparable to published research, thereby validating the model. [42, 43]

Joint angles were compared to values reported in published research. Hemmerich reported flexion, external rotation, and adduction angles between of 153-157°, 9-11°, and 6-8°, respectively for squatting and 144-155°, 11-12°, and 7-10°, respectively for kneeling near full flexion. [44] Although flexion angles agree with those in their research, the adduction and

external rotation angles are somewhat larger than those in this study. This is mostly due to the differences in kneeling postures. In this study, Subject 1 performed kneeling near full flexion with their buttocks resting on their heels. Subject 2 did not rest their buttocks on their heels, but did kneel with their buttocks over their heels. In Hemmerich's study, subjects performed kneeling in full flexion without placing any weight on their heels and in a more upright posture. This may have resulted in increased abduction moments. Also the orientation of the feet may have created external rotation in their subjects, and internal rotation in Subjects 1 and 2 of this study. Knee rotations also agree with the 11.1 ± 6.7° of internal rotation found in passive knee flexion to 150°. [45] The knee joint angles when standing were also compared to published research. The right knee had an included angle of 174-179° with 2.4-2.6° valgus and .1-.8° of internal rotation, which is comparable to published research. [46]

7.0 DISCUSSION

This discussion section includes the sensitivity of the computational model to the model parameters and knee joint center location which are important factors when applying this model to future research. The effect of kneepads on the force and moments, subject variability, the implications of findings, and the advancements are explained. Also the limitations of this study which may restrict the extent to which these findings may be generalized are discussed.

7.1 KNEEPADS

Kneepads were not expected to significantly affect the knee joint angles and no statistically significant differences in joint angles were found within subjects. Kneepads were also not expected to significantly affect the forces at the knee. However, they were expected to affect the moments at the knee joint. The knee pad was expected to change the location of the center of pressure at the knee, which would change the moment arm of that force, thereby affecting the moment. Although no statistically significant differences were found between kneepad states, there were differences in the transverse moments which may have been caused by the kneepads. In Subject 1 when kneeling near 90° flexion without kneepads, the moment arm of the ground-reaction force at the knee was [-.014, .031, -.025], contributing 2.14 Nm to the internal rotational moment of the knee. When wearing kneepads this moment arm changed to [-.036, .04, -.021],

contributing 9.86 Nm. This implies that the COP of the ground-reaction force at the knee was shifted 2.2 mm medially when wearing kneepads. Forces were also different between kneepad states [66.87, -308.91, -40.73] N and [51.25, -327.52, -47.90] N without and with kneepads, respectively. However, the differences in lateral forces and distal distances accounted for merely .07 Nm of the 7.72 Nm increase in internal rotational moment. The other 7.65 Nm were due to the proximal force and its medial distance from the KJC. Similar changes in moments were seen in the kneeling on one knee and kneeling near full flexion postures for this subject. The design of the kneepad (articulating with a hard, contoured outer shell) is thought to have contributed to this increase in transverse moment. This magnitude of torque may introduce significant changes in the stresses and strains experienced by the internal stabilizing structures of the knee.

7.2 MODEL SENSITIVITY

7.2.1 Model Parameters

The developed computational model showed variations in sagittal moments as a result of changes in moment arms and forces. No variation in moment arm or force changed the moment by an order of magnitude, however some variations were sufficient to change the interpretation of the moment from flexion to extension. When analyzing the kneeling on one knee and kneeling near 90° flexion postures, the model was most sensitive to the location of the ground reaction force at the knee, doubling or tripling the moment when varying the location by 3 cm. In kneeling near full flexion and squatting, the model was most sensitive to the moment arm of the

thigh-calf contact force, in some cases doubling the knee moment due to varying the COP by 3 cm. Sagittal moments changed from flexion to extension when the z-component of the COP at the knee was increased by 3 cm for kneeling near 90° flexion and kneeling on one knee. All efforts should be made to ensure proper positioning of all moment arms, especially the moment arms of the thigh-calf contact force and the COP of the force at the knee to reduce errors associated with these model parameters.

7.2.2 Knee Joint Center Location

Variations in knee joint center location had large effects on the moment calculations and varied between postures. Internal rotational moments were increased when the KJC was moved laterally or posteriorly. Flexion moments were decreased when the KJC was moved posteriorly and increased when the KJC was moved proximally. Adduction moments were increased when the KJC was moved laterally or proximally. Due to the high sensitivity of moments to KJC location care must be taken to ensure proper placement of surface markers on the medial and lateral epicondyles. In this study the location of the medial and lateral epicondyle was marked while the subject sat with their knee at 90°. One subject was responsible for palpating and marking these anatomic landmarks. It is possible that changes in marker placement may create error in moment calculations and joint angles. However the error in marker placement is expected to be less than the 3 cm variations studied.

7.3 SUBJECT VARIABILITY

While the model was only tested on two subjects, there did appear to be differences between them. Subject 1 and Subject 2 showed significantly different joint angles, forces, and moments during kneeling. This variability may be due to their difference in stature as well as kneeling postures. Inclusion of more subjects will be needed to determine any anthropometric effects on the results with and without kneepads.

A comparison of the two subjects yields some insights into potential inter-subject variability. When kneeling near 90° flexion both subjects had similar forces and moments with kneepads. Without kneepads, Subject 2 was in a more flexed posture creating increased flexion moments. When kneeling on one knee Subject 1 was in a more upright posture, kneeling close to 90° with the right leg and the supporting left leg. Subject 2 was in a much more crouched posture with joint angles closer to that in full flexion and squatting. This caused increased ground reaction forces at the foot and decreased ground reaction forces at the knee leading to increased flexion moments in Subject 2. When kneeling near full flexion, Subject 1 sat on their heels with their feet rotated laterally. Subject 2 did not sit on their heel and kept their feet in a vertical position with minimal rotation. This accounted for the decreased varus angles and frontal and transverse moments of Subject 2. When squatting, Subject 1 had a wider stance which may have accounted for the adduction moments created compared to the abduction moments in Subject 2.

7.4 LIMITATIONS

The limitations of the developed model are associated with the complexity of kneeling near the end range of flexion, as well as with the use of inverse dynamics. The assumptions necessary to use the computational model may not be valid in all circumstances. The state of the joint cartilage may null the assumption of a frictionless joint, as degenerative cartilage increases the friction at the articulating surfaces. Also, the distribution of mass in any body segment is not uniform nor is it concentrated at one location. The external applied forces are not applied directly to the tibia, thereby causing forces which may not be linearly related to the resulting moments due to tissue deformation. The patellar tendon and tibial tubercle may change the center of pressure location and magnitudes of forces applied to the tibia during kneeling thereby affecting the force and moment calculations.

The use of reflective markers to track the motion of palpable landmarks may have introduced some sources of error. Motion of the skin to which reflective markers are attached, also known as soft tissue artifact, strongly affects the estimation of joint angles characterized by small range of motion. [47] Markers were placed on the medial and lateral epicondyles of the femur while the subject was in a standing T-pose for 5 seconds. These markers were then removed and re-created in data analysis. Motion of these markers was minimal with standard deviations between .9 and 1.8 mm for Subject 1. Therefore the relative motion of these markers with respect to the anatomical landmarks is not expected to introduce error in the knee joint center estimation.

A Tekscan ClinSeat® system was used to measure the thigh-calf and heel-gluteus contact forces. The use of this type of system, a system which uses resistive technology, has been found to introduce creep in the measurement of static forces varying the force measurements by -10 %

to +20 %. [48] Also calibration of this system may reduce the accuracy and repeatability of its measurements. [49] The recommended calibration is performed by applying a constant pressure to the sensor by sitting on the sensor, thereby calibrating the sensor to bodyweight. It is possible that the values reported from this system are inaccurate due to the method of calibration. Every attempt was made to ensure repeatability of the calibrated values. One researcher calibrated the system by sitting on the sensor atop a table with their left leg on the portion of the sensor that is placed under the subject's lower leg.

Along with the issues associated with measuring the contact forces, there are limitations associated with the representation of these forces in the model. The thigh-calf and heel-gluteus contact forces were represented as single resultant forces, however these contact forces are more complex. Thigh-calf contact creates a pressure distribution which has higher contact pressures closer to the popliteal region. Heel-gluteus contact creates a pressure distribution with pressures highest in the middle of the contact area. Both contact pressures create tissue deformation which may act to distribute the axial load in multiple directions. However, the system used to measure these contact force was only capable of measuring axial pressure. Therefore shear forces resulting from this contact were neglected from the model. Also due to the design of the pressure sensor, the full contact surface could not be measured. The active sensing units on the ClinSeat® system are located approximately 1.5 cm away from the top of the sensor. This distance was accounted for when determining the center of pressures of these contact forces. However the lack of pressure measurements in these areas decreased the measured total force. This decrease in force may have been significant to increase the calculated flexion moments, thereby creating an over-estimation in sagittal moments. Future studies on thigh-calf contact should use measurement tools capable of quantifying the entire contact area and measuring

forces in multiple axes. Also, when modeling this contact tissue deformation should be accounted for to reduce error in frontal and transverse moments.

Knee joint center location estimates have been shown to affect the interpretation of joint moments in gait studies with small moment magnitudes. [50] Although the sagittal joint moments in this model are of a higher magnitude, there are limitations associated with the KJC location used in this model. Femoral "roll-back" causes the KJC to move during knee flexion. In the lateral compartment the femur moves 20 mm posterior from 0 to 120° of flexion and an additional 10 mm when kneeling into a deep squat. In the medial compartment there is little to no movement until 120° of flexion when there is a posterior displacement of 9 mm. [51] This movement accounts for the increase in varus/valgus and internal/external rotations at higher knee flexion. In this study, imaging techniques were not employed which would have been necessary to determine the location of the knee joint center for all joint postures studied. Future studies on knee biomechanics in which imaging techniques can be engaged should account for this change in joint center location.

Thigh-calf and heel-gluteus contact force measurements were made for kneeling near full flexion and squatting, prior to collection of motion capture and force data. Although this was necessary to determine the moments for these postures, it neglects the possibility that similar contact may be present in the other postures. Since subjects were not given specific instructions on kneeling postures, it is possible that they may assume the kneeling near 90° flexion and kneeling on one knee posture with higher flexion angles than anticipated. When kneeling on one knee and kneeling near 90° flexion without kneepads, Subject 2 had included angles similar to those during their squatting postures. These angles introduced thigh-calf contact which was not measured nor accounted for in the computational model. Neglecting this contact resulted in

over-estimations of the flexion moments for these postures. In future studies it may be necessary to instruct subjects to assume very specific postures such that all contact forces may be accounted for and comparisons may be made between kneepads states.

Due to the small sample size, N=2, concrete conclusions cannot be drawn on the forces and moments created in restricted postures. The small sample size creates a very small power and statistics may not have been appropriate to show significant differences between postures or subjects. Although data from two subjects were presented, the goal of this master's thesis project was the development of the model to determine the external forces and moments, and not to characterize the forces and moments seen in kneeling and squatting. In the future this model will be applied to data from a much larger dataset and resulting forces and moments will be published.

7.5 IMPLICATIONS OF FINDINGS

Kneeling and squatting create tibial loading conditions which differ substantially from standing. Increased flexion moments open the anterior aspects of the joint, increasing the loads to the posterior tibia. Adduction moments open the medial joint space, stressing the medial soft tissues and applying increased loads to the lateral compartment of the tibia. Abduction moments open the lateral joint space, increasing stresses in lateral tissues and loads transmitted to the medial compartment. Internal and external rotational moments will increase the loading to the medial and lateral compartments of the knee, respectively. These complex loading conditions were created in the kneeling postures in this study. The implications of these increased joint torques on the muscles, ligaments, meniscus, and articular cartilage are presented.

7.5.1 Muscles Activity

To resist the externally applied forces and moments and reduce tibial translations, active and passive internal knee stabilizers are used. Active knee stabilizers include the muscles and tendons and passive stabilizers include the ligaments and soft tissues. In this study muscle activity was not used as a model input and it is expected that the results would change significantly if muscle activity were included in the force and moment calculations. When considering the forces applied to the knee, it is assumed that the quadriceps muscle group is responsible for resisting the externally applied flexion moments. However, although not included in the results, EMG data of the quadriceps and hamstrings muscles were collected. Results showed minimal activity, < 5% MVC, in these static postures. This implies that the knee stability is mostly achieved by the passive stabilizers. Thus, the implications of this study are that the high moments and forces calculated in the model may be transferring to the passive stabilizers of the knee. The transference of the results of this model to the FEM model being developed as part of the larger effort within the project will give an understanding of the magnitude of these passive tissue loads.

7.5.2 Ligament Recruitment

The passive stability due to the ligaments and soft tissues will depend on knee orientation and loading. Studies of passive knee motion reveal interesting findings of the recruitment patterns of the passive knee stabilizers when kneeling near 90° flexion. Internal rotation recruits the anterior bundles of the anterior cruciate ligament (ACL) along with the anterior and posterior bundles of the posterior cruciate ligament (PCL) with primary stability from the posterior

bundles of the PCL. The application of a posterior force recruits, the anterior bundles of the PCL and MCL. [52] Although adduction moments are generally stabilized primarily by the ACL and the MCL, when kneeling near 90° flexion the MCL is the primary stabilizer with secondary restraint from the PCL. [53, 54] Kneeling near 90° flexion and kneeling on one knee created posterior forces along with adduction and internal rotational moments in both subjects. To restrict tibial translations and rotations when in these postures, the PCL is expected to be the primary stabilizer with assistance from the ACL and MCL. A maximum 500 N posterior force, 10 Nm adduction moment, and 11 Nm external rotational moment were applied to the tibia when kneeling in these postures. Fukuda and colleagues found an in-situ ACL force of 19.5 N when subjected to a 10 Nm adduction moment at 90° flexion. [55] Carlin and colleagues found an in-situ PCL force of 95 N when subjected to a 100 N posterior force at 90° flexion. [56] If findings from these in-situ studies are correlated to the forces and moments from this study, it is not expected that kneeling postures requiring approximately 90° of knee flexion (kneeling near 90° flexion and kneeling on one knee) will cause detriment to the ligaments.

The stability of the knee in the fully flexed postures of kneeling near full flexion and squatting is more complicated. In vivo studies of weight bearing knees in high flexion show that up to 120° the PCL plays a major role in providing knee stability from posterior translation. [52, 57] However, in high flexion (above 120°) the PCL does not contribute substantially to knee stability. It is believed that the posterior soft tissues of the knee (posterior horns of the meniscus, posterior capsule, hamstrings muscles, fat, and skin) not the PCL provide stability in high flexion. [58]

7.5.3 Meniscal Loading

During walking 70% of the total knee load is distributed to the medial compartment of the knee joint. [59] This increases the load on the medial meniscsus. When an abduction moment is added to the tibia, the load increases. In the kneeling near 90° flexion and kneeling on one knee postures, the contact area between the tibia and the meniscus is thought to be sufficient to withstand the forces created under these conditions without damage. However, with increasing joint flexion, as in the kneeling near full flexion and squatting postures, there is posterior translation of the tibia. This translation is also accompanied by the posterior translation of the meniscus with the lateral horn translating more than the medial horn. This posterior translation functions to increase the contact area between the tibia and the meniscus and may play a crucial role in distributing compressive loads in full flexion. [60] Compared to extension, in high flexion, the contact between the tibia and the femur occur at the posterior aspects of the knee, decreasing the contact area resulting in increased stresses in the posterior meniscus.

Along with knee flexion playing a major role in the loads and contact areas of the meniscus, adduction and abduction moments contribute to the loading of the meniscus. Adduction and abduction moments increase loading to the lateral and medial compartments of the knee. [61] In Subject 1, adduction moments were created when kneeling near full flexion and squatting. The adduction moments in postures with high knee flexion may cause detrimental effects on the lateral meniscus. The adduction moments which were as much as 16 Nm in conjunction with the posterior forces of up to 120 N, increase the shear loads transmitted to the meniscus. In Subject 2, abduction moments increased the loading to the medial meniscus. The moments which were up to 21 Nm in combination with 160 N posterior forces, increased the shear load to the meniscus. These loads are then transferred to the articular cartilage with

maximal shear stress occurring at the cartilage-bone interface away from the center of contact. [62] This creates areas of high stress on the articular cartilage and when sustained for prolonged periods could lead to the deterioration of the meniscus and articular cartilage damage.

7.5.4 Osteoarthritis Progression

Articular cartilage damage may occur as a result of biological and mechanical factors. Two forms of articular cartilage damage occur from loading. Type 1 articular cartilage damage is characterized by damage without disruption of the underlying bone or calcified cartilage layer. Type 2 damage is characterized by bone fracture with or without damage to the overlying cartilage. [63] Excessive shear stress, tensile stress, and principal strain have been suggested as mechanisms of articular cartilage damage. [63 - 65] Thambyah and colleagues found articular cartilage stresses of 14 MPa during gait and these stresses increased by more than 80% when in deep flexion. This increased stress reached the damage limit of the cartilage and was thought to increase the risk of articular cartilage damage. [66] Thus, the implications are that the high moments and forces associated with kneeling near full flexion and squatting may cause excessive stress on the articular cartilage of the tibiofemoral joint thereby increasing the risk for knee osteoarthritis.

7.5.5 Postures Associated with Osteoarthritis

Epidemiologic studies have determined postures associated with increased prevalence of knee osteoarthritis including squatting, kneeling, stair climbing, side-knee bending, and sitting crossed-legged. [17, 32] Stair climbing produces forces and moments greater than that during

walking. [67, 68] Stair descent creates flexion, varus/valgus, and external rotational moments greater than level walking or stair ascent, making it a more stressful activity. [68] In this study all postures created frontal moments and posterior forces greater than standing. Although kneeling with joint flexion close to 90° is not expected to cause damage to the articular cartilage, it is expected that postures with higher joint flexion will. The combination of increased frontal moments, increased posterior force, and high knee flexion, create high loads on the medial and lateral posterior compartments of the knee and may create the biomechanical stresses necessary to initiate the developments and progression of medial and lateral compartment knee osteoarthritis.

7.6 ADVANCEMENTS

The developed computational model accounts for the contact between the heel and the gluteal muscles which until now, had been neglected from other models. Thigh-calf contact has been shown to significantly affect the forces in the quadriceps and it is expected that the heel-gluteus contact will have similar effects on muscle force estimations. In this study the heel-gluteus contact force was 54 N which was almost half of the 124 N thigh-calf contact force. If a force of 124 N is significant to effect muscle force estimations than an additional force of 54 N should also be significant to affect these forces.

Results of the sensitivity analysis revealed that the location of the thigh-calf contact has a large effect on the knee moments when kneeling near full flexion and squatting. Although when using this model this may be a limitation, when considering the design of interventions this may be an important factor. Early interventions to reduce the stresses and strains at the knee joint

have focused on the outside of the knee, i.e. knee pads. However, slightly changing postures or the distribution of body weight may be useful. Newer devices should consider maximizing the thigh-calf and heel-gluteus contact forces in hopes of distributing more body weight along the lower leg, thereby creating an extensor moment to stabilize the knee joint in full flexion. It was also found that the kneepad acted to change the COP of the force at the knee by as much as 2.9 cm in the medial/lateral direction which created an 8 Nm increase in transverse moments. This increase in rotational moment may be detrimental to the internal knee structures. It therefore becomes important to consider the effect of new devices on the transverse and frontal moments of the knee which are often neglected due to their smaller magnitudes when compared to sagittal moments.

8.0 FUTURE WORK

In the near future the forces and moments determined using this model will be used as inputs into a finite element model of the knee. In addition to motion capture, force data, and thigh-calf and heel-gluteus contact measurements, electromyography and knee surface pressure data were collected as part of this project. Electromyography was used to determine which muscles were active during different stages of kneeling, crawling, and stooping. Subjects were also instrumented with a custom designed pressure sensor on their right knee under their kneepad. This pressure sensor was used to measure the pressure distributions at the patella, patellar tendon, and tibial tubercle with and without kneepads. Also a second commonly used kneepad with a different design (non-articulating, soft outer shell) was used. Gaining a better understanding of the pressures, forces, and moments at the knee joint and in the internal stabilizing structures, will allow development of better solutions to the complex knee problems facing many low-seam coal miners. The end-product of this project will be the design of a new intervention which will be effective in reducing the stress and strains in the internal knee structures caused by frequent and prolonged kneeling, stooping, and crawling.

9.0 CONCLUSION

In this work a 3-D computational model based on inverse dynamics and segment coordinate systems was developed in MATLAB to determine the joint angles and net force and moments applied to the knee in static kneeling postures. This model was custom fitted to each subject and based off their individual anthropometry, ground reaction forces, thigh-calf contact force, and heel-gluteus contact force measurements. Sensitivity analysis revealed that varying the location of the knee joint center affected the sagittal, frontal, and transverse moments in all postures. In some cases the interpretation of the joint moment changed due to varying the KJC by 3 cm. This model was developed for use on a much larger dataset currently being collected. However, data from two subjects were presented in this paper. These subjects revealed that kneeling creates high external knee joint moments which may be as much as 10 to 40 times that during quiet standing. There were also large variations in the moments between postures and kneepads states. Postures requiring larger flexion angles generally created larger flexion moments at the knee. The more upright postures of kneeling near 90° flexion and kneeling on one knee created increased posterior forces, up to 500N. Also ankle positioning appeared to play a large role in the increased frontal moments associated with kneeling. One subject internally rotated their ankles when kneeling which caused large knee adduction moments, up to 16 Nm. This increased adduction moment in combination with increased posterior forces, increases the forces applied to the medial compartment of the knee and may be significant to create cartilage

damage. The other subject had large abduction moments, 21 Nm, when squatting which increased loading to the lateral aspects of the meniscus. It was also found that the kneepad used in this study changed the center of pressure of the force at the knee, in some cases increasing the transverse moment by as much as 8 Nm. A larger dataset will be necessary to determine the effect of these kneeling postures on the internal structures of the knee. However, this study suggests that kneeling increases the flexion moments applied to the knee as well as the adduction moments and posterior forces and may be significant to initiate meniscal and articular cartilage damage.

APPENDIX

MATLAB SOFTWARE

The MATLAB® software developed to determine the net forces, net moments, and joint angles at the knee consists of eight MATLAB® files. Three files are used to calculate the forces, moments, and angles. The other files are necessary for importing data and exporting results. The three files: transform_m2a_shank_thigh.m, knee_angle.m, and forces_moments.m, perform all necessary calculations and are included in this appendix.

A.1 TRANSFORM_M2A_SHANK_THIGH.M

Transform_m2a_shank_thigh.m is used to calculate the transformation matrix from the global coordinate system to the anatomical coordinate system, the transformation matrix from the global coordinate system to the measured coordinate system, and the transformation matrix from the measured coordinate system to the anatomical coordinate system.

```
function [filename]=transform_m2a(results_directory)

%%%%%%%%%%%%%%%%%%%%%%%%%%%% transform_m2a.m %%%%%%%%%%%%%%%%%%%%%%%%%%%%%%%%
%%%%
%%%% This function is designed to produce the transformation matrix from
%%%% testing coordinates to anatomical coordinates. This function uses
%%%% only the anatomical (calibration) data
%%%%    1. Assign data to specific markers
%%%%   Part 1 - Shank
%%%%    2. Determine the anatomical coordinate system for shank and
%%%%       calculate the transformation matrix from global to anatomical
%%%%       coordinates
%%%%    3. Determine the measured/testing coordinate system and calculate
%%%%       the transformation matrix from global to measured
%%%%       coordinates
%%%%    4. Determine the transformation matrix from measured to anatomical
%%%%       and get the mean value of this matrix
%%%%   Part 2 - Thigh
%%%%    2-4 for thigh
%%%%    5. Save transformation matrix TMAshank to mat file
%%%%
%%%%        Jonisha Pollard, JPollard@cdc.gov, 8/19/08
%%%%%%%%%%%%%%%%%%%%%%%%%%%%%%%%%%%%%%%%%%%%%%%%%%%%%%%%%%%%%%%%%%%%%%%%%%%%

%% Load Anatomical Data
    cd(results_directory);
    load anatomical.mat

%% Determine length of data
   [n o]=size(anatomical_data);

%% 1. Assign data to specific markers
    right_knee=anatomical_data(:,45:47);
    right_knee_medial=anatomical_data(:,78:80);
    right_ankle=anatomical_data(:,51:53);
    right_ankle_medial=anatomical_data(:,81:83);
    right_shank=anatomical_data(:,48:50);
    right_shank_front=anatomical_data(:,111:113);
    right_shank_rear=anatomical_data(:,114:116);
    right_thigh=anatomical_data(:,42:44);
    right_thigh_front=anatomical_data(:,93:95);
    right_thigh_rear=anatomical_data(:,96:98);

    left_knee=anatomical_data(:,63:65);
    left_knee_medial=anatomical_data(:,84:86);
    left_ankle=anatomical_data(:,69:71);
    left_ankle_medial=anatomical_data(:,87:89);
    left_shank=anatomical_data(:,66:68);
    left_shank_front=anatomical_data(:,120:122);
    left_shank_rear=anatomical_data(:,123:125);
    left_thigh=anatomical_data(:,60:62);
    left_thigh_front=anatomical_data(:,102:104);
    left_thigh_rear=anatomical_data(:,105:107);

    rasis=anatomical_data(:,33:35);
    lasis=anatomical_data(:,36:38);
```

```
    %% Determine location of joint centers in global coordinates
    AJC=(right_ankle + right_ankle_medial)/2;  % Global Right AJC
    KJC=(right_knee + right_knee_medial)/2;    % Global Right KJC

    AJC_L=(left_ankle + left_ankle_medial)/2;  % Global Left AJC
    KJC_L=(left_knee + left_knee_medial)/2;    % Global Left KJC


    % Global HJC Calculation. Bells method
    % Leardini et al. 1999, Bell et al. 1990
    HJC_origin=(lasis+rasis)/2;
    PW=abs(lasis(:,1)-rasis(:,1)); % inter Asis distance
    HJC(:,1)=HJC_origin(:,1)+.36*PW;
    HJC(:,2)=HJC_origin(:,2)-.19*PW;
    HJC(:,3)=HJC_origin(:,3)-.3*PW;

    HJC_L(:,1)=HJC_origin(:,1)-.36*PW;
    HJC_L(:,2)=HJC_origin(:,2)-.19*PW;
    HJC_L(:,3)=HJC_origin(:,3)-.3*PW;



%%%%%%%%%%%%%%%%%%%%%% Part 1 - Shank %%%%%%%%%%%%%%%%%%%%%%%%%
%% 2. Determine anatomical coordinate system for shank and calculate
%%    transformation matrix from global to anatomical coordinates

        % All coordinate systems were chosen such that hey align with the
        % Global coordinate system at Standard anatomical position

        % Global & Anatomical Coordinate Systems
        % x is medial/lateral
        % y is anterior/posterior
        % z is superior/inferior

    % Right
        for i=1:n
            r1=KJC-AJC;                              % local z-axis
            r2=right_knee - right_knee_medial;       % in x-direction
            r3=cross(r1,r2);                         % local y-axis
            r4=cross(r3,r1);                         % local x-axis
            x(i,:)=r4(i,:)/norm(r4(i,:));
            y(i,:)=r3(i,:)/norm(r3(i,:));            % rotation matrix
            z(i,:)=r1(i,:)/norm(r1(i,:));
        end

       TGAshank=zeros(4,4,n);
        for i=1:n
            TGAshank(1,:,i)=[1 0 0 0];
            TGAshank(2:4,1,i)=KJC(i,:);      %right KJC is origin
            TGAshank(2:4,2,i)=x(i,:);
            TGAshank(2:4,3,i)=y(i,:);
            TGAshank(2:4,4,i)=z(i,:);
        end
```

```
    clear r1 r2 r3 r4 x y z         % clear variables

    % calculate AJC and KJC in anatomical shank coordinates
    for i=1:n
        G_ajc(i,2:4)=AJC(i,:);
        G_ajc(:,1)=1;
        G_kjc(i,2:4)=KJC(i,:);
        G_kjc(:,1)=1;
        asAJC_all(i,:)=inv(TGAshank(:,:,i))*G_ajc(i,:)';   %Shank AJC
        asKJC_all(i,:)=inv(TGAshank(:,:,i))*G_kjc(i,:)';   %Shank KJC
    end

    asAJC=mean(asAJC_all(:,2:4));
    asKJC=mean(asKJC_all(:,2:4));    % verified to equal [0 0 0]


% Left
    for i=1:n
        r1=KJC_L-AJC_L;                          % local z-axis
        r2=left_knee_medial - left_knee;         % in x-direction
        r3=cross(r1,r2);                         % local y-axis
        r4=cross(r3,r1);                         % local x-axis
        x(i,:)=r4(i,:)/norm(r4(i,:));
        y(i,:)=r3(i,:)/norm(r3(i,:));            % rotation matrix
        z(i,:)=r1(i,:)/norm(r1(i,:));
    end

  TGAshank_L=zeros(4,4,n);
    for i=1:n
        TGAshank_L(1,:,i)=[1 0 0 0];
        TGAshank_L(2:4,1,i)=KJC_L(i,:);      % left KJC is origin
        TGAshank_L(2:4,2,i)=x(i,:);
        TGAshank_L(2:4,3,i)=y(i,:);
        TGAshank_L(2:4,4,i)=z(i,:);
    end

    clear r1 r2 r3 r4 x y z         % clear variables

    % calculate AJC and KJC in anatomical shank coordinates
    for i=1:n
    G_ajc_L(i,2:4)=AJC_L(i,:);
    G_ajc_L(:,1)=1;
    G_kjc_L(i,2:4)=KJC_L(i,:);
    G_kjc_L(:,1)=1;
    asAJC_all_L(i,:)=inv(TGAshank_L(:,:,i))*G_ajc_L(i,:)'; %Shank AJC
    asKJC_all_L(i,:)=inv(TGAshank_L(:,:,i))*G_kjc_L(i,:)'; %Shank KJC
    end

    asAJC_L=mean(asAJC_all_L(:,2:4));
    asKJC_L=mean(asKJC_all_L(:,2:4));

%% 3. Determine the measured coordinate system for shank and calculate the
%%    transformation matrix from global to measured
      %% Global & Anatomical Coordinate Systems
```

```
        %% x is medial/lateral
        %% y is anterior/posterior
        %% z is superior/inferior

    % Right shank
        for i=1:n
            r1=right_shank-right_shank_front;            % local z-axis
            r2=right_shank_front - right_shank_rear;     % in y direction
            r3=cross(r2,r1);                             % local x-axis
            r4=cross(r1,r3);                             % local y-axis
            x(i,:)=r3(i,:)/norm(r3(i,:));
            y(i,:)=r4(i,:)/norm(r4(i,:));                % rotation matrix
            z(i,:)=r1(i,:)/norm(r1(i,:));
        end


        TGMshank=zeros(4,4,n);

        for i=1:n
            TGMshank(1,:,i)=[1 0 0 0];
            TGMshank(2:4,1,i)=right_shank_front(i,:);       % origin
            TGMshank(2:4,2,i)=x(i,:);
            TGMshank(2:4,3,i)=y(i,:);
            TGMshank(2:4,4,i)=z(i,:);
        end
        clear r1 r2 r3 r4 x y z         % clear variables

    % Left shank
        for i=1:n
            r1=left_shank-left_shank_front;            % local z-axis
            r2=left_shank_front - left_shank_rear;     % in y direction
            r3=cross(r2,r1);                           % local x-axis
            r4=cross(r1,r3);                           % local y-axis
            x(i,:)=r3(i,:)/norm(r3(i,:));
            y(i,:)=r4(i,:)/norm(r4(i,:));              % rotation matrix
            z(i,:)=r1(i,:)/norm(r1(i,:));
        end

        TGMshank_L=zeros(4,4,n);

        for i=1:n
            TGMshank_L(1,:,i)=[1 0 0 0];
            TGMshank_L(2:4,1,i)=left_shank_front(i,:);       % origin
            TGMshank_L(2:4,2,i)=x(i,:);
            TGMshank_L(2:4,3,i)=y(i,:);
            TGMshank_L(2:4,4,i)=z(i,:);
        end

       clear r1 r2 r3 r4 x y z         % clear variables

%% 4. Calculate transformation matrix from measured to anatomical coords
     % Right
        TMAs_alldata=zeros(4,4,n);    % TMAshank for all data points
        for i=1:n
            TMAs_alldata(:,:,i)=inv(TGMshank(:,:,i))*TGAshank(:,:,i);
```

```
        end

        % calculate the mean of TMAshank_alldata
        TMAshank=zeros(4,4);
        for i=2:4
            for j=1:4
                TMAshank(i,j)=mean(TMAs_alldata(i,j,:));
                TMAshank(1,1)=1;
                TMAshank(1,2:4)=0;
            end
        end

     % Left
        TMAs_alldata_L=zeros(4,4,n);    % TMAshank_L for all data points
        for i=1:n
            TMAs_alldata_L(:,:,i)=inv(TGMshank_L(:,:,i))*TGAshank_L(:,:,i);
        end

        % calculate the mean of TMAshank_L_alldata
        TMAshank_L=zeros(4,4);
        for i=2:4
            for j=1:4
                TMAshank_L(i,j)=mean(TMAs_alldata_L(i,j,:));
                TMAshank_L(1,1)=1;
                TMAshank_L(1,2:4)=0;
            end
        end


%%%%%%%%%%%%%%%%%%%%%% Part 2 - Thigh %%%%%%%%%%%%%%%%%%%%%%%%%
%% 2. Determine anatomical coordinate system for thigh and calculate
%%    transformation matrix from global to anatomical coords
        %% Global & Anatomical Coordinate Systems
        %% x is medial/lateral
        %% y is anterior/posterior
        %% z is superior/inferior

    % Right Thigh
        for i=1:n
            r1=HJC-KJC;                              % local z-axis
            r2=right_knee - right_knee_medial;       % in x-direction
            r3=cross(r1,r2);                         % local y-axis
            r4=cross(r3,r1);                         % local x-axis
            x(i,:)=r4(i,:)/norm(r4(i,:));
            y(i,:)=r3(i,:)/norm(r3(i,:));            % rotation matrix
            z(i,:)=r1(i,:)/norm(r1(i,:));
        end

       TGAthigh=zeros(4,4,n);
        for i=1:n
            TGAthigh(1,:,i)=[1 0 0 0];
            TGAthigh(2:4,1,i)=HJC(i,:);      %right HJC is origin
            TGAthigh(2:4,2,i)=x(i,:);
            TGAthigh(2:4,3,i)=y(i,:);
            TGAthigh(2:4,4,i)=z(i,:);
```

```
 end

clear r1 r2 r3 r4 x y z         % clear variables

% calculate HJC and KJC in anatomical thigh coordinates
for i=1:n
    G_hjc(i,2:4)=HJC(i,:);
    G_hjc(:,1)=1;
    G_kjc(i,2:4)=KJC(i,:);
    G_kjc(:,1)=1;
    atHJC_all(i,:)=inv(TGAthigh(:,:,i))*G_hjc(i,:)';   %Thigh HJC
    atKJC_all(i,:)=inv(TGAthigh(:,:,i))*G_kjc(i,:)';   %Thigh KJC
end

atHJC=mean(atHJC_all(:,2:4)); % verified to equal [0 0 0]
atKJC=mean(atKJC_all(:,2:4));


% Left Thigh
 for i=1:n
     r1=HJC_L-KJC_L;                          % local z-axis
     r2=left_knee_medial - left_knee;         % in x-direction
     r3=cross(r1,r2);                         % local y-axis
     r4=cross(r3,r1);                         % local x-axis
     x(i,:)=r4(i,:)/norm(r4(i,:));
     y(i,:)=r3(i,:)/norm(r3(i,:));            % rotation matrix
     z(i,:)=r1(i,:)/norm(r1(i,:));
 end

TGAthigh_L=zeros(4,4,n);
 for i=1:n
     TGAthigh_L(1,:,i)=[1 0 0 0];
     TGAthigh_L(2:4,1,i)=HJC_L(i,:);      %left HJC is origin
     TGAthigh_L(2:4,2,i)=x(i,:);
     TGAthigh_L(2:4,3,i)=y(i,:);
     TGAthigh_L(2:4,4,i)=z(i,:);
 end

clear r1 r2 r3 r4 x y z         % clear variables

% calculate HJC and KJC in anatomical thigh coordinates
for i=1:n
G_hjc_L(i,2:4)=HJC_L(i,:);
G_hjc_L(:,1)=1;
G_kjc_L(i,2:4)=KJC_L(i,:);
G_kjc_L(:,1)=1;
atHJC_all_L(i,:)=inv(TGAthigh_L(:,:,i))*G_hjc_L(i,:)'; %Thigh HJC
atKJC_all_L(i,:)=inv(TGAthigh_L(:,:,i))*G_kjc_L(i,:)'; %Thigh KJC
end

atHJC_L=mean(atHJC_all_L(:,2:4)); % verified to equal [0 0 0]
atKJC_L=mean(atKJC_all_L(:,2:4));
```

```
%% 3. Determine the measured coordinate system for thigh and calculate
%%    transformation from global to measured
        %% Global & Anatomical Coordinate Systems
        %% x is medial/lateral
        %% y is anterior/posterior
        %% z is superior/inferior

   % Right
        for i=1:n
            r1=right_thigh-right_thigh_front;           % local z-axis
            r2=right_thigh_front-right_thigh_rear;      % in y direction
            r3=cross(r2,r1);                            % local x-axis
            r4=cross(r1,r3);                            % local y-axis
            x(i,:)=r3(i,:)/norm(r3(i,:));
            y(i,:)=r4(i,:)/norm(r4(i,:));               % rotation matrix
            z(i,:)=r1(i,:)/norm(r1(i,:));
        end

        TGMthigh=zeros(4,4,n);

        for i=1:n
            TGMthigh(1,:,i)=[1 0 0 0];
            TGMthigh(2:4,1,i)=right_thigh_front(i,:); %origin
            TGMthigh(2:4,2,i)=x(i,:);
            TGMthigh(2:4,3,i)=y(i,:);
            TGMthigh(2:4,4,i)=z(i,:);
        end

        clear r1 r2 r3 r4 x y z         % clear variables

 % Left
         for i=1:n
            r1=left_thigh-left_thigh_front;           % local z-axis
            r2=left_thigh_front-left_thigh_rear;      % in y direction
            r3=cross(r2,r1);                          % local x-axis
            r4=cross(r1,r3);                          % local y-axis
            x(i,:)=r3(i,:)/norm(r3(i,:));
            y(i,:)=r4(i,:)/norm(r4(i,:));             % rotation matrix
            z(i,:)=r1(i,:)/norm(r1(i,:));
        end

        TGMthigh_L=zeros(4,4,n);

        for i=1:n
            TGMthigh_L(1,:,i)=[1 0 0 0];
            TGMthigh_L(2:4,1,i)=left_thigh_front(i,:); %origin
            TGMthigh_L(2:4,2,i)=x(i,:);
            TGMthigh_L(2:4,3,i)=y(i,:);
            TGMthigh_L(2:4,4,i)=z(i,:);
        end

        clear r1 r2 r3 r4 x y z         % clear variables

%% 4. Calculate transformation matrix from measured to anatomical coords
```

```
    % Right
        TMAt_alldata=zeros(4,4,n);   % TMAthigh for all data point
        for i=1:n
            TMAt_alldata(:,:,i)=inv(TGMthigh(:,:,i))*TGAthigh(:,:,i);
        end

        % calculate the mean of TMAthigh_alldata
        TMAthigh=zeros(4,4);
        for i=2:4
            for j=1:4
                TMAthigh(i,j)=mean(TMAt_alldata(i,j,:));
                TMAthigh(1,1)=1;
                TMAthigh(1,2:4)=0;
            end
        end

     % Left
        TMAt_alldata_L=zeros(4,4,n);   % TMAthigh for all data point
        for i=1:n
            TMAt_alldata_L(:,:,i)=inv(TGMthigh_L(:,:,i))*TGAthigh_L(:,:,i);
        end

        % calculate the mean of TMAthigh_alldata
        TMAthigh_L=zeros(4,4);
        for i=2:4
            for j=1:4
                TMAthigh_L(i,j)=mean(TMAt_alldata_L(i,j,:));
                TMAthigh_L(1,1)=1;
                TMAthigh_L(1,2:4)=0;
            end
        end

%%  5. Save transformation matrixes KJC, AJC and HJC mat file
    save anatomical.mat TMAshank TMAthigh asAJC TMAshank_L TMAthigh_L ...
         asAJC_L -append


end % end of function transform_m2a.m
```

A.2 KNEE ANGLE.M

Knee_angle.m is used to calculate the orientation of the knee joint. Using Euler angle decomposition, with a Euler order of X'y'z", the included joint angle, the angle of varus/valgus, and the angle of internal/external rotation are calculated.

```
function knee_angle(posture, results_directory)


%%%%%%%%%%%%%%%%%%%%%%%%%%% knee_angle.m %%%%%%%%%%%%%%%%%%%%%%%%%%%
%%%% This function is designed to determine the knee angle by calculating
%%%% the angle between the thigh coordinate system and the shank coordinate
%%%% system.
%%%% 1. Load testing marker data and assign data to specific markers
%%%% 2. Determine measured coordinate system for shank and thigh
%%%% 3. Calculate anatomical coordinate system from measured system and
%%%%    determine transformation from thigh to shank Tts
%%%% 4. Decompose transformation matrix for Euler angles
%%%% 5. Save joint angles to *posture*.mat
%%%%
%%%%         Jonisha Pollard, JPollard@cdc.gov, 7/23/08
%%%%%%%%%%%%%%%%%%%%%%%%%%%%%%%%%%%%%%%%%%%%%%%%%%%%%%%%%%%%%%%%%%%%%%%

cd(results_directory)
load(posture)          %load mat file with data for specific postures
load anatomical        %load mat file with anatomical markers and TMAshank

%%  1. Load testing marker data and assign data to specific markers
    [n a]=size(testing_data);
    right_shank=testing_data(:,39:41);
    right_shank_rear=testing_data(:,48:50);
    right_shank_front=testing_data(:,45:47);
    right_thigh=testing_data(:,27:29);
    right_thigh_front=testing_data(:,33:35);
    right_thigh_rear=testing_data(:,36:38);

    left_shank=testing_data(:,81:83);
    left_shank_rear=testing_data(:,90:92);
    left_shank_front=testing_data(:,87:89);
    left_thigh=testing_data(:,69:71);
    left_thigh_front=testing_data(:,75:77);
    left_thigh_rear=testing_data(:,78:80);
```

```
%% 2. Determine measured coordinate system for shank and thigh
        %% Global Coordinate System
        %% x is medial/lateral
        %% y is anterior/posterior
        %% z is superior/inferior

    % Right shank
        for i=1:n
            r1=right_shank-right_shank_front;            % local z-axis
            r2=right_shank_front - right_shank_rear;     % in y direction
            r3=cross(r2,r1);                             % local x-axis
            r4=cross(r1,r3);                             % local y-axis
            x(i,:)=r3(i,:)/norm(r3(i,:));
            y(i,:)=r4(i,:)/norm(r4(i,:));                % rotation matrix
            z(i,:)=r1(i,:)/norm(r1(i,:));
        end

        TGMshank=zeros(4,4,n);
        for i=1:n
            TGMshank(1,:,i)=[1 0 0 0];
            TGMshank(2:4,1,i)=right_shank_front(i,:); % origin
            TGMshank(2:4,2,i)=x(i,:);
            TGMshank(2:4,3,i)=y(i,:);
            TGMshank(2:4,4,i)=z(i,:);
        end

    clear r1 r2 r3 r4 x y z

   % Right thigh
       for i=1:n
            r1=right_thigh-right_thigh_front;            % local z-axis
            r2=right_thigh_front-right_thigh_rear;       % in y direction
            r3=cross(r2,r1);                             % local x-axis
            r4=cross(r1,r3);                             % local y-axis
            x(i,:)=r3(i,:)/norm(r3(i,:));
            y(i,:)=r4(i,:)/norm(r4(i,:));                % rotation matrix
            z(i,:)=r1(i,:)/norm(r1(i,:));
        end

        TGMthigh=zeros(4,4,n);
        for i=1:n
            TGMthigh(1,:,i)=[1 0 0 0];
            TGMthigh(2:4,1,i)=right_thigh_front(i,:);      % origin
            TGMthigh(2:4,2,i)=x(i,:);
            TGMthigh(2:4,3,i)=y(i,:);
            TGMthigh(2:4,4,i)=z(i,:);
        end

        clear r1 r2 r3 r4 x y z

    % Left shank
        for i=1:n
            r1=left_shank-left_shank_front;            % local z-axis
            r2=left_shank_front - left_shank_rear;     % in y direction
```

```
            r3=cross(r2,r1);                                % local x-axis
            r4=cross(r1,r3);                                % local y-axis
            x(i,:)=r3(i,:)/norm(r3(i,:));
            y(i,:)=r4(i,:)/norm(r4(i,:));                   % rotation matrix
            z(i,:)=r1(i,:)/norm(r1(i,:));
        end

        TGMshank_L=zeros(4,4,n);
        for i=1:n
            TGMshank_L(1,:,i)=[1 0 0 0];
            TGMshank_L(2:4,1,i)=left_shank_front(i,:); % origin
            TGMshank_L(2:4,2,i)=x(i,:);
            TGMshank_L(2:4,3,i)=y(i,:);
            TGMshank_L(2:4,4,i)=z(i,:);
        end

        clear r1 r2 r3 r4 x y z


% Left thigh
       for i=1:n
            r1=left_thigh-left_thigh_front;             % local z-axis
            r2=left_thigh_front-left_thigh_rear;        % in y direction
            r3=cross(r2,r1);                            % local x-axis
            r4=cross(r1,r3);                            % local y-axis
            x(i,:)=r3(i,:)/norm(r3(i,:));
            y(i,:)=r4(i,:)/norm(r4(i,:));               % rotation matrix
            z(i,:)=r1(i,:)/norm(r1(i,:));
        end

        TGMthigh_L=zeros(4,4,n);
        for i=1:n
            TGMthigh_L(1,:,i)=[1 0 0 0];
            TGMthigh_L(2:4,1,i)=left_thigh_front(i,:);      % origin
            TGMthigh_L(2:4,2,i)=x(i,:);
            TGMthigh_L(2:4,3,i)=y(i,:);
            TGMthigh_L(2:4,4,i)=z(i,:);
        end

        clear r1 r2 r3 r4 x y z


%%  3. Calculate anatomical coordinate system from measured system and
%%  determine transformation from thigh to shank Tts

        for i=1:n
         % Right
            TGAshank(:,:,i)=TGMshank(:,:,i)*TMAshank;
            TGAthigh(:,:,i)=TGMthigh(:,:,i)*TMAthigh;
            Tts(:,:,i)=inv(TGAthigh(:,:,i))*TGAshank(:,:,i);
            Rts(:,:,i)=Tts(2:4,2:4,i);     % rotation matrix

         % Left
            TGAshank_L(:,:,i)=TGMshank_L(:,:,i)*TMAshank_L;
            TGAthigh_L(:,:,i)=TGMthigh_L(:,:,i)*TMAthigh_L;
```

```
            Tts_L(:,:,i)=inv(TGAthigh_L(:,:,i))*TGAshank_L(:,:,i);
            Rts_L(:,:,i)=Tts_L(2:4,2:4,i);     % rotation matrix
        end

%%  4. Decompose transformation matrix for Euler angle

% Global Coordinate System
        % 1st axis - flexion/ext - X
        % 2nd axis - varus/valgus - Y
        % 3rd axis - inversion/eversion - Z
        % Euler order Xy'z''


        for i=1:n
            z_angle(i,:)=((180/pi) * atan2(-Rts(1,2,i),Rts(1,1,i)));
            x_angle(i,:)=180 + ((180/pi) * atan2(-Rts(2,3,i),Rts(3,3,i)));
            y_angle(i,:)=((180/pi) * atan2(cos(z_angle(i,:))*Rts(1,3,i),...
                         Rts(1,1,i)));

            z_angle_L(i,:)=((180/pi) * atan2(-Rts_L(1,2,i),Rts_L(1,1,i)));
            x_angle_L(i,:)=180 + ((180/pi) * atan2(-Rts_L(2,3,i), ...
                           Rts_L(3,3,i)));
            y_angle_L(i,:)=((180/pi) * atan2(cos(z_angle_L(i,:)) ...
                           *Rts_L(1,3,i),Rts_L(1,1,i)));
        end

%%  5. Save angles

   save(posture,'x_angle','y_angle','z_angle','Tts','TGAthigh',...
       'TGAshank','x_angle_L','y_angle_L','z_angle_L','Tts_L', ...
       'TGAthigh_L','TGAshank_L','-append')

  end         % end of function knee_angle.m
```

A.3 FORCES_MOMENTS.M

Forces_moments.m is used to calculate the net external forces, moments, and moment contributions at the knee joint in the global coordinate system. The forces and moments are then transformed into the anatomical coordinate system.

```
function forces_moments(weight, height, posture, results_directory)

%%%%%%%%%%%%%%%%%%%%%%%%%%%% forces_moments.m %%%%%%%%%%%%%%%%%%%%%%%%%%%%
%%%% This function is designed to calculate the net forces and moments at
%%%% the knee joint for squatting and full flexion
%%%% 1. Load testing marker data and assign data to specific markers
%%%% 2. Load force plate data
%%%% 3. Determine measured coordinate system for shank
%%%% 4. Get anatomical shank coordinates from testing coordinates
%%%% 5. Determine COP and weight of segments and joint rotation centers
%%%% 6. Calculate the joint reactive forces at the right knee in Global
%%%%    coordinates
%%%% 7. Calculate the moment at the right knee in Global coordinates
%%%% 8. Calculate forces and moments in Anatomical coordinates
%%%% 9. Normalize forces and moments
%%%% 10. Saves forces and moments to *posture*.mat
%%%%
%%%%        Jonisha Pollard, JPollard@cdc.gov, 7/23/08
%%%%%%%%%%%%%%%%%%%%%%%%%%%%%%%%%%%%%%%%%%%%%%%%%%%%%%%%%%%%%%%%%%%%%%%%%%%

cd(results_directory)
load(posture)     %load mat file with data for specific postures
load anatomical   %load mat file with anatomical markers and TMAshank

%%  1. Load testing marker data and assign data to specific markers
    [n a]=size(testing_data);
    right_shank=testing_data(:,39:41);
    right_shank_rear=testing_data(:,48:50);
    right_shank_front=testing_data(:,45:47);


%%  2. Load force plate data
    F1=forces_data(:,2:4);
    COP1=forces_data(:,5:7);
    F2=forces_data(:,9:11);
    COP2=forces_data(:,12:14);
```

```
%%  3. Determine measured coordinate system for shank

    %% Global Coordinate System
    %% x is medial/lateral
    %% y is anterior/posterior
    %% z is superior/inferior

    for i=1:n
        r1=right_shank-right_shank_front;            % local z-axis
        r2=right_shank_front - right_shank_rear;     % in y direction
        r3=cross(r2,r1);                             % local x-axis
        r4=cross(r1,r3);                             % local y-axis
        x(i,:)=r3(i,:)/norm(r3(i,:));
        y(i,:)=r4(i,:)/norm(r4(i,:));                % rotation matrix
        z(i,:)=r1(i,:)/norm(r1(i,:));
    end


    TGMshank=zeros(4,4,n);
    for i=1:n
        TGMshank(1,:,i)=[1 0 0 0];
        TGMshank(2:4,1,i)=right_shank_front(i,:);      % origin
        TGMshank(2:4,2,i)=x(i,:);
        TGMshank(2:4,3,i)=y(i,:);
        TGMshank(2:4,4,i)=z(i,:);
    end


%%  4. Get anatomical shank coordinates from measured coordinates

    for i=1:n
        TGAshank(:,:,i)=TGMshank(:,:,i)*TMAshank;   % transformation matrix
        RGAshank(:,:,i)=TGAshank(2:4,2:4,i);        % rotation matrix
    end

%%  5. Determine COM, COP, joint rotation centers, and contact forces in
%%        global coordinates

    for i=1:n
    % calculate location of AJC and KJC in global coordinates
       g_AJC(i,:)=TGAshank(:,:,i)*[1 asAJC]';
       g_KJC(i,:)=TGAshank(:,:,i)*[1 0 0 0]';% KJC is origin of ACS [0 0 0]

    % calculate thigh-calf and heel-gluteus COP in global coordinates
    %  these contact forces are located along the z axis of the shank coord
       COP_tc(i,:)=TGAshank(:,:,i)*[1 0 0 -tc_dist]';
       COP_hg(i,:)=TGAshank(:,:,i)*[1 0 0 -hg_dist]';

    % Thigh-calf and Heel-gluteus contact forces in global coordinate system
        gtc_cont(i,:)=RGAshank(:,:,i)*[0 tc_cont 0]';
        ghg_cont(i,:)=RGAshank(:,:,i)*[0 hg_cont 0]';
    end
```

```
    gAJC=g_AJC(:,2:4); %eliminate '1' in 1st col
    gKJC=g_KJC(:,2:4);
    COPtc=COP_tc(:,2:4);
    COPhg=COP_hg(:,2:4);

    % Lower leg COM and weight are modified from Clauser et al 1969 and
    % Hinrichs 1990
    % 47.5% of distance from proximal to distal
    COM_lowleg=gAJC+.525*(gKJC - gAJC);
    W_lowleg=zeros(n,3);
    W_lowleg(:,3)=-.058*weight;



%% 6. Calculate the joint reactive forces at the right knee in Global
%% Coordinates

    % Sum of all forces at knee should equal zero
    % Sum forces = Force_r_knee + F1 + F2 + W_lowleg + tc + hg = 0
    %             Knee reaction force = -(F1 + F2 + W_lowleg + tc + hg)
    % Force imposed on knee =F1 + F2 + W_lowleg + tc + hg

    % Force imposed on Knee (reaction force will be -)
    Fknee= F1 + F2 + W_lowleg + gtc_cont + ghg_cont;


%% 7. Calculate moment at the right knee joint in Global Coordinates
    % Sum of all moments at knee should equal zero
    % Moments will be calculated using the vector cross product

    % Sum of Moments at knee= Knee_reaction_Moment+ MF1 + MF2 + Mlowleg + Mtc
    %                           + Mhg= 0
    %       Knee_reaction_Moment = -(MF1 + MF2 + Mlowleg + Mtc + Mhg)
    %      Moment imposed on knee= MF1 + MF2 + Mlowleg + Mtc + Mhg

    % moment arm vectors in m
        r_lowleg=(COM_lowleg-gKJC)/1000;
        r_FP1=(COP1-gKJC)/1000;
        r_FP2=(COP2-gKJC)/1000;
        r_tc=(COPtc-gKJC)/1000;
        r_hg=(COPhg-gKJC)/1000;

    % calculate moments in N-m
       for i=1:n
           M_lowleg(i,:)=cross(r_lowleg(i,:),W_lowleg(i,:));
           MF1(i,:)=cross(r_FP1(i,:),F1(i,:));
           MF2(i,:)=cross(r_FP2(i,:),F2(i,:));
           Mhg(i,:)=cross(r_hg(i,:),ghg_cont(i,:));
           Mtc(i,:)=cross(r_tc(i,:),gtc_cont(i,:));
       end

       % Moment imposed on knee. Muscle moment will be (-)
        Mknee= M_lowleg + MF1 + MF2 + Mtc + Mhg;
```

```
%%  8. Calculate forces, moments, and moment arms in Anatomical shank
coordinates
    % Forces
    % FA = [RGA]^-1 * FG
       for i=1:n
            aF1(i,:)=inv(RGAshank(:,:,i))*F1(i,:)';
            aF2(i,:)=inv(RGAshank(:,:,i))*F2(i,:)';
            aW_lowleg(i,:)=inv(RGAshank(:,:,i))*W_lowleg(i,:)';

         % COP locations
            aCOPlowleg(i,:)=(inv(TGAshank(:,:,i))*[1 COM_lowleg(i,:)]');
            aCOP1(i,:)=(inv(TGAshank(:,:,i))*[1 COP1(i,:)]');
            aCOP2(i,:)=(inv(TGAshank(:,:,i))*[1 COP2(i,:)]');
       end

       atc_cont=zeros(n,3);
       atc_cont(:,2)=tc_cont;
       ahg_cont=zeros(n,3);
       ahg_cont(:,2)=hg_cont;

       % Total Force imposed on Knee
       aFknee= aF1+ aF2 + aW_lowleg + atc_cont + ahg_cont;

       % Moment arms
       ar_lowleg=aCOPlowleg(:,2:4)/1000;
       ar_FP1=aCOP1(:,2:4)/1000;
       ar_FP2=aCOP2(:,2:4)/1000;
       ar_tc=[0 0 -tc_dist]/1000;
       ar_hg=[0 0 -hg_dist]/1000;


       % Moments
      for i=1:n
           aM_lowleg(i,:)=cross(ar_lowleg(i,:),aW_lowleg(i,:));
           aMF1(i,:)=cross(ar_FP1(i,:),aF1(i,:));
           aMF2(i,:)=cross(ar_FP2(i,:),aF2(i,:));
           aMhg(i,:)=cross(ar_hg,[0 hg_cont 0]);
           aMtc(i,:)=cross(ar_tc,[ 0 tc_cont 0]);
      end



            % Moment imposed on knee
             aMknee=aM_lowleg + aMF1 + aMF2 + aMtc + aMhg;
```

```
%% 9. Normalize forces and moments
       % forces will be normalized to body weight
       % moments will be normalized to bodyweight*height

      % Global forces
       nF1=(100/weight)*F1;
       nF2=(100/weight)*F2;
       nW_lowleg=(100/weight)*W_lowleg;
       ngtc_cont=(100/weight)*gtc_cont;
       nghg_cont=(100/weight)*ghg_cont;
       nFknee=(100/weight)*Fknee;

      % Anatomical Forces
       naF1=(100/weight)*aF1;
       naF2=(100/weight)*aF2;
       naW_lowleg=(100/weight)*aW_lowleg;
       natc_cont=(100/weight)*atc_cont;
       nahg_cont=(100/weight)*ahg_cont;
       naFknee=(100/weight)*aFknee;

       nMF1=(100/(weight*height))*MF1;
       nMF2=(100/(weight*height))*MF2;
       nM_lowleg=(100/(weight*height))*M_lowleg;
       nMtc=(100/(weight*height))*Mtc;
       nMhg=(100/(weight*height))*Mhg;
       nMknee=(100/(weight*height))*Mknee;

       naMF1=(100/(weight*height))*aMF1;
       naMF2=(100/(weight*height))*aMF2;
       naMtc=(100/(weight*height))*aMtc;
       naMhg=(100/(weight*height))*aMhg;
       naMknee=(100/(weight*height))*aMknee;
       naM_lowleg=(100/(weight*height))*aM_lowleg;

%%  10. Save forces and moments to *posture*.mat
    cd(results_directory)
    save(posture,'F1','F2', 'W_lowleg', 'gtc_cont', 'ghg_cont', 'Fknee',...
       'nF1', 'nF2','nW_lowleg', 'ngtc_cont', 'nghg_cont','nFknee', ...
       'aF1','aF2', 'aW_lowleg', 'atc_cont', 'ahg_cont', 'aFknee',...
       'naF1', 'naF2','naW_lowleg', 'natc_cont', 'nahg_cont', 'naFknee',...
       'r_FP1', 'r_FP2','r_lowleg',  'r_tc', 'r_hg', ...
       'ar_FP1', 'ar_FP2', 'ar_lowleg', 'ar_tc', 'ar_hg', ...
       'MF1', 'MF2', 'M_lowleg', 'Mtc', 'Mhg', 'Mknee', ...
       'nMF1', 'nMF2', 'nM_lowleg', 'nMtc', 'nMhg', 'nMknee', ...
       'aMF1', 'aMF2', 'aM_lowleg', 'aMtc', 'aMhg', 'aMknee', ...
       'naMF1', 'naMF2', 'naM_lowleg', 'naMtc', 'naMhg', 'naMknee', ...
       '-append')



  end         % end of function forces_moments.m
```

BIBLIOGRAPHY

[1] Lawrence RC, Felson DT, Helmich CG, et al. Estimates of the Prevalence of Arthritis and Other Rheumatic Conditions in the United States. Part 2. Arthritis & Rheumatism. 2008;58(1):26-35

[2] Maetzel A, Li LC, Pencharz J, Tomlinson F, Bombardier C. The economic burden associated with osteoarthritis, rheumatoid arthritis, and hypertension: A comparative study. Ann Rheum Dis, 2004;63(4):395- 401

[3] Anderson JJ & Felson DT. Factors Associated With Osteoarthritis of the Knee in the First National Health and Nutrition Examination Survey (HANES I). American Journal of Epidemiology. 1988;128(1):179-189

[4] Kivimäki J, Riihimäki H, Hänninen K. Knee disorders in carpet and floor layers and painters. Scand J Work Environ Health. 1992;18(5):310-316

[5] Zelle J, Barink M, Loeffen R, De Waal Malefijt M, Verdonschot N. Thigh-calf contact force measurements in deep knee flexion. Clinical Biomechanics. 2007;22:821-826

[6] Welsh RP. Knee Joint Structure and Function. Clinical Orthopaedics and Related Research. 1980;147;7-14

[7] Baker P, Reading I, Cooper C, and Coggon D. Knee disorders in the general population and their relation to occupation. Occup Environ med. 2003;60;794-797

[8] Jensen, Lilli K. Knee-straining work activities, self-reported knee disorders and radiographically determined knee osteoarthritis. Scand J Work Environ Health. 2005;31 suppl 2:68-74

[9] Sharrard, WJW. Pressure Effects on the Knee in Kneeling Miners. Ann R Coll Surg Engl. 1965;36;309-24

[10] Sharrard WJW, Liddell FDK. Injuries to the Semilunar cartilage of the knee in miners. Brit J. Industr. Med, 1962;19;195-202

[11] http://www.tri-countyortho.com/mmg/pated/knee_problems/anatomy/quads.jpg Retrieved April 17, 2008

[12] Seedhom BB, Dowson D, Wright, V. Proceedings: Functions of the menisci: a preliminary work. Ann Rheum Dis 1974:33(1):111

[13] Macquet Paul G, Van de Berg André J, Simonet Jacques C. Femorotibial Weight-Bearing Areas. The Journal of Bone and Joint Surgey. 1975;57-A(6):766-771

[14] Smith JP, Barrett GR. Medial and Lateral Meniscal Tear Patterns in Anterior Cruciate Ligament-Deficient Knees. American Journal of Sports Medicine. 2001;29(4):415-419

[15] Meister K, Indelicato PA, Spanier S, Franklin J, Batts J. A Comparison of Histologic Differences in Meniscal Tissue Between Tears in Anterior Cruciate Ligament-Intact and Anterior Cruciate Ligament-Deficient Knees. The American Journal of Sports Medicine. 2005;32(6):1479-1483

[16] Hoshino A, Wallace WA. Impact-Absorbing Properties of the Human Knee. The Journal of Bone and Joint Surgery. 1987;69-B;807-811

[17] Tangtrakulwanich B, Chongsuvivatwong V, Geater AF. Habitual Floor Activities Increase Risk of Knee Osteoarthritis. Clinical Orthopaedics and Related Research. 2006;454:147-154

[18] National Institute of Arthritis and Musculoskeletal and Skin Diseases (NIAMS). www.niams.nih.gov

[19] Lavender SA and Andersson GBJ. Ergonomic principles applied to prevention of injuries to the lower extremity. In W Karwowski & WS Marras (Eds.), The Occupational Ergonomics Handbook. (pp 883-893). Boca Raton, FL. CRC Press

[20] United States Bureau of Labor Statistics. Incidence rates for nonfatal occupational injuries and illnesses involving days away from work per 10,000 full-time workers by part of body and selected sources of injury or illness, 2006.

[21] McMillan G, Nichols L. Osteoarthritis and meniscus disorders of the knee as occupational diseases of miners. Occup Environ Med. 2005;62:567-575

[22] Drosos GI, Pozo JL. The causes and mechanisms of meniscal injuries in the sporting and non-sporting environment in an unselected population. The Knee. 2004;11:143-149

[23] Smillie IS. Injuries to the knee joint. Edinburgh, London and New York: Churchill Livingstone, 1978. pp. 71-149

[24] Baratz ME, Fu FH, Mengato R. Meniscal tears: the effect of meniscectomy and of repair on intrarticular contact areas and stress in the human knee: a preliminary report. Am J Sports Med 1986:14(4):270

[25] Hawkins A, McNicholas MJ. Meniscectomy and arthritis. CME Orthopaedics 2001;2(2):51-56

[26] Biswal S, Hastie T, Andriacchi TP, Bergman GA, et al. Risk Factors for Progressive Cartilage Loss in the Knee. Arthritis & Rheumatism. 2002;46(11):2884-2892

[27] Hunter DJ, Zhang YQ, Niu JB, et al. The Association of Meniscal Pathologic Changes with Cartilage Loss in Symptomatic Knee Osteoarthritis. Arthritis & Rheumatism. 2006;54(3):795-801

[28] Felson DT & Zhang Y. An Update on the Epidemiology of Knee and Hip Osteoarthritis with a View to Prevention. Arthritis & Rheumatism. 1998;41(8):1343-1355

[29] Anderson JA. Athrosis and its relation to work. Scand J Work Environ Health. 1984;10(6):429-433

[30] Kellgren JH & Lawrence JS. Rheumatism In Miners Part II: X-Ray Study. Brit. J. Industr. Med. 1952;9:197-207

[31] Cooper C, McAlindon T, Coggon D, Egger P, Dieppe P. Occupational activity and osteoarthritis of the knee. Ann Rheum Dis. 1994;53:90-93

[32] Zhang Y, Hunter DJ, Nevitt MC, Xu L et al. Association of squatting with increased prevalence of radiographic Tibiofemoral knee osteoarthritis. The Beijing osteoarthritis study. Arthritis & Rheumatism. 2004;50(4):1187-1192

[33] Dahlvist NJ, Mayo P, Seedhom BB. Forces during squatting and rising from a deep squat. Eng Med 1982;11:69-76

[34] Perry J, Antonelli D, Ford W. Analysis of knee-joint forces during flexed-knee stance. J Bone Joint Surg Am. 1975;57:961-967

[35] Nagura T, Dyrby CO, Alexander EJ, Andriacchi TP. Mechanical loads at the knee joint during deep flexion. Journal of Orthopaedic Research. 2002;20:881-886

[36] Caruntu DI, Hefzy MS, Goel VK, Goitz HT, Dennis MJ, Agrawal V. Modeling the Knee Joint in Deep Flexion: ”Thigh and Calf” Contact. Summer Bioengineering Conference. June 25-29, 2003. Key Biscayne, Florida

[37] Winter, D.A. (1990). Biomechanics and motor control of human movement. Wiley, New York

[38] Bell AL, Brand RA, Pedersen DR. A comparison of the accuracy of several hip center location prediction methods. Journal of Biomechanics. 1990;23;617-621

[39] Clauser CE, JT McConville, JM Young (1969) Weight,volume and center of mass of segments of the human body. AMRL-TR-69-70, Wright-Patterson Air Force Base, Ohio.

[40] Hinrichs, RN. Adjustments to the segment center of mass proportions of Clauser et al. (1969). J Biomechanics. 1990;23(9):949-951

[41] Moisio KC, Summer DR, Shott S, Hurwitz DE. Normalization of joint moments during gait: a comparison of two techniques. Journal of Biomechanics. 2003;36:599-603

[42] Allard P, Lachance R, Aissaoui R, Duhaime M. Simultaneous bilateral 3-D able-bodied gait. Human Movement Science. 1996;15:327-346

[43] Eng JJ & Winter DA. Kinetic analysis of the lower limbs during walking: what information can be gained from a three-dimensional model? Journal of Biomechanics. 1995;28(6):753-758

[44] Hemmerich A, Brown H, Smith S, Marthandam SSK, and Wyss UP. Hip, knee, and ankle kinematics of high range of motion activities of daily living. Journal of Orthopaedic Research. 2006;24(4):770-781

[45] Li G, Zayontz S, DeFrate LE, et al. Kinematics of the knee at high flexion angles: an in vitro investigation. Journal of Orthopaedic Research. 2004;22(1):90-95

[46] Kadaba MP, Ramakrishnan HK, Wootten ME. Measurement of lower extremity kinematics during level walking. Journal of Orthopaedic Research. 1990; 8:383-392

[47] Stagni R, Fantozzi S, Capello A. Propagation of anatomical landmark misplacement to knee kinematics: Performance of single and double calibration. Gait & Posture. 2006;24:137-141

[48] Martinelli L, Hurschler C, Rosenbaum D. Comparison of capacitive versus resistive joint contact stress sensors. Clinical and Orthopaedics and related research. 2006;447:214-220

[49] Morin EI, Bryant JT, Reid SA, Whiteside RA. Calibration Issues of Tekscan Systems for Human Pressure Assessment. Presented at RTO HFM Specialists Meeting on "Soldier Mobility: Innovations in Load Carriage Systems Design and Evaluation". Kingston, Canada, June 27-29, 2000

[50] Holden JP, Stanhope SJ. The effect of variation in knee center location estimates on net knee joint moments. Gait & Posture.1998;7;1-6

[51] Williams A, Logan M. Understanding Tibio-Femoral motion. The Knee. 2004;11;81-88

[52] Blankevoort L, Huiskes R, de Lange A. Recruitment of Knee Joint Ligaments. Journal of Biomechanical Engineering. 1991;113:94-103

[53] Matsumoto H, Suda Y, Otani T, Niki Y et al. Role of the anterior cruciate ligament and the medial collateral ligament in preventing valgus instability. Journal of Orthopaedic Sciences. 2001;6(1):28-32

[54] Toshiyuki M, Hideo M, Yasumfumi S, Yoshihiro S et al. Function of the knee cruciate ligaments as restraints on varus-valgus torque. Simultaneous measurement of tension along the ACL and PCL. Proceedings of Annual Meeting of Japanese Society for Orthopaedic Biomechanics. 1999;20:151-156

[55] Fukuda Y, Woo S, Loh J, Tsuda E et al. A quantitative analysis of valgus torque on the ACL: a human cadaveric study. Journal of Orthopaedic Research. 2003;21(6):1107-1112

[56] Carlin GJ, Livesay GA, Harner CD et al. In-situ Forces in the Human Posterior Cruciate Ligament in Response to Posterior Tibial Loading. Annals of Biomedical Engineering. 1996;24(2):193-197

[57] Papannagari R, DeFrate LE, Nha KW et al., Function of posterior cruciate ligament bundles during in vivo knee flexion. American Journal of Sports Medicine. 2007;38:1507-1512

[58] Li G, Most E, DeFrate LE, et al. Effect of posterior cruciate ligament on posterior stability of the knee in high flexion. Journal of Biomechanics. 2004;37(5):779-783

[59] Hurwitz DE, Sumner DR, Andriachhi TP, and Sugar DA. Dynamic knee loads during gait predict proximal tibial bone distribution. Journal of Biomechanics. 1998;31:423-430

[60] Yao J, Lancianese SL, Hovinga KR, Lee J, Lerner AL. Magnetic resonance image analysis of meniscal and tibio-menisco-femoral contact in deep knee flexion. Journal of Orthopaedic Research. 2008;26(5):673-684

[61] Schipplein OD and Adriacchi TP. Interaction between active and passive knee stabilizers during level walking. Journal of Orthopaedic Research. 1991;9:113-119

[62] Wilson W, Rietbergen B, Donkelaar CC, and Huiskes R. Pathways of load-induced cartilage damage causing cartilage degeneration in the knee after meniscectomy. Journal of Biomechanics. 2003;36:845-851

[63] Atkinson TS, Haut RC, and Altiero NJ. Impact-induced fissuring of articular cartilage: An investigation of failure criteria. Journal of Biomechanical Engineering. 1998:120:181-187

[64] Eberhardt A, Lewis J, and Keer L. Normal contact of elastic spheres with two elastic layers as a model of joint articulation. Journal of Biomechanical Engineering. 1991:113:410-417

[65] Kelly PA and O'Connor JJ. Transmission of Rapidly Applied Loads Through Articular Cartilage Part 1: Uncracked Cartilage. Jounral of Engineering Medicine. 1996;210:27-37

[66] Thambyah A, Goh JCH, Das De S. Contact stresses in the knee joint in deep flexion. Medical Engineering and Physics. 2005;27:329-335

[67] Costigan PA, Deluzio KJ, Wyss UP. Knee and hip kinetics during normal stair climbing. Gait and Posture. 2002;16:31-37

[68] Kaufman KR, Hughes C, Morrey BF, Morrey M, An K. Gait characteristics of patients with knee osteoarthritis. Journal of Biomechanics. 2001;34:907-915